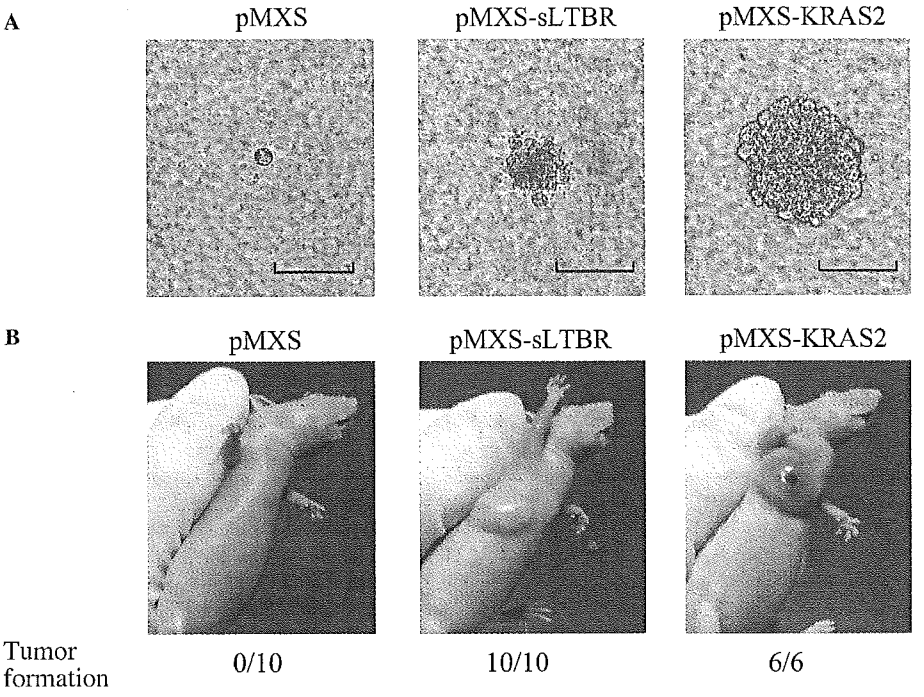

Fig. 4. Transforming activity of short-type LTBR. (A) Focus formation assay. 3T3 cells infected either with empty retrovirus (pMXS) or with retroviruses encoding short-type LTBR (pMXS-sLTBR) or activated KRAS2 (pMXS-KRAS2) were seeded into soft agar and incubated for 2 weeks. Scale bars, 100 μm. (B) Tumorigenicity assay. Cells infected as in (A) were injected into the shoulder of nude mice and tumor formation was examined after 3 weeks. The frequency of tumor formation determined is indicated.

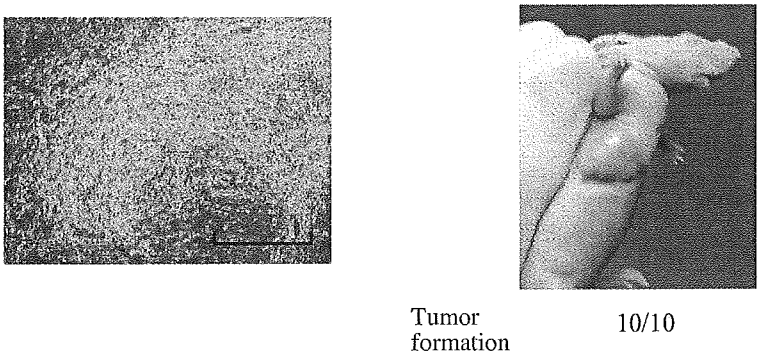

Fig. 5. Transforming activity of full-length LTBR. The transforming activity of a retroviral vector encoding full-length (wild-type) LTBR was evaluated by the focus formation assay (left) or the in vivo tumorigenicity assay (right). Scale bar, 1 mm.

of the protein. It is thus likely that LTBR exerts its oncogenic function in a tissue- and context-dependent manner. As shown here for PDC, it will be important to determine whether LTBR also contributes to the mechanism of transformation in other human malignancies.

Acknowledgments

This work was supported in part by a grant for Third-Term Comprehensive Control Research for Cancer from the Ministry of Health, Labor, and Welfare of Japan as well as by a grant for "High-Tech Research Center" Project for Private Universities: Matching Fund Subsidy (2002–2006) from the Ministry of Education, Culture, Sports, Science and Technology of Japan.

References

[1] S. Rosewicz, B. Wiedenmann, Pancreatic carcinoma, Lancet 349 (1997) 485–489.
[2] P.C. Bornman, I.J. Beckingham, Pancreatic tumours, Br. Med. J. 322 (2001) 721–723.
[3] M. Tada, M. Omata, M. Ohto, Clinical application of ras gene mutation for diagnosis of pancreatic adenocarcinoma, Gastroenterology 100 (1991) 233–238.
[4] S.R. Bramhall, The use of molecular technology in the differentiation of pancreatic cancer and chronic pancreatitis, Int. J. Pancreatol. 23 (1998) 83–100.

[5] G. Schneider, J.T. Siveke, F. Eckel, R.M. Schmid, Pancreatic cancer: basic and clinical aspects, Gastroenterology 128 (2005) 1606–1625.
[6] A. Yanagisawa, K. Ohtake, K. Ohashi, M. Hori, T. Kitagawa, H. Sugano, Y. Kato, Frequent c-Ki-ras oncogene activation in mucous cell hyperplasias of pancreas suffering from chronic inflammation, Cancer Res. 53 (1993) 953–956.
[7] S.A. Aaronson, Growth factors and cancer, Science 254 (1991) 1146–1153.
[8] M.A. Frohman, M.K. Dush, G.R. Martin, Rapid production of full-length cDNAs from rare transcripts: amplification using a single gene-specific oligonucleotide primer, Proc. Natl. Acad. Sci. USA 85 (1988) 8998–9002.
[9] P.D. Crowe, T.L. VanArsdale, B.N. Walter, C.F. Ware, C. Hession, B. Ehrenfels, J.L. Browning, W.S. Din, R.G. Goodwin, C.A. Smith, A lymphotoxin-β-specific receptor, Science 264 (1994) 707–710.
[10] J.L. Browning, I.D. Sizing, P. Lawton, P.R. Bourdon, P.D. Rennert, G.R. Majeau, C.M. Ambrose, C. Hession, K. Miatkowski, D.A. Griffiths, A. Ngam-ek, W. Meier, C.D. Benjamin, P.S. Hochman, Characterization of lymphotoxin-αβ complexes on the surface of mouse lymphocytes, J. Immunol. 159 (1997) 3288–3298.
[11] W.R. Force, B.N. Walter, C. Hession, R. Tizard, C.A. Kozak, J.L. Browning, C.F. Ware, Mouse lymphotoxin-β receptor. Molecular genetics, ligand binding, and expression, J. Immunol. 155 (1995) 5280–5288.
[12] A. Futterer, K. Mink, A. Luz, M.H. Kosco-Vilbois, K. Pfeffer, The lymphotoxin β receptor controls organogenesis and affinity maturation in peripheral lymphoid tissues, Immunity 9 (1998) 59–70.
[13] R.M. Locksley, N. Killeen, M.J. Lenardo, The TNF and TNF receptor superfamilies: integrating mammalian biology, Cell 104 (2001) 487–501.
[14] J.L. Browning, K. Miatkowski, I. Sizing, D. Griffiths, M. Zafari, C.D. Benjamin, W. Meier, F. Mackay, Signaling through the lymphotoxin β receptor induces the death of some adenocarcinoma tumor lines, J. Exp. Med. 183 (1996) 867–878.
[15] I.A. Rooney, K.D. Butrovich, A.A. Glass, S. Borboroglu, C.A. Benedict, J.C. Whitbeck, G.H. Cohen, R.J. Eisenberg, C.F. Ware, The lymphotoxin-β receptor is necessary and sufficient for LIGHT-mediated apoptosis of tumor cells, J. Biol. Chem. 275 (2000) 14307–14315.
[16] P. Yu, Y. Lee, W. Liu, R.K. Chin, J. Wang, Y. Wang, A. Schietinger, M. Philip, H. Schreiber, Y.X. Fu, Priming of naive T cells inside tumors leads to eradication of established tumors, Nat. Immunol. 5 (2004) 141–149.
[17] T. Hehlgans, B. Stoelcker, P. Stopfer, P. Muller, G. Cernaianu, M. Guba, M. Steinbauer, S.A. Nedospasov, K. Pfeffer, D.N. Mannel, Lymphotoxin-β receptor immune interaction promotes tumor growth by inducing angiogenesis, Cancer Res. 62 (2002) 4034–4040.

HUMAN GENE THERAPY 16:1212–1218 (October 2005)

Technical Report

Large-Scale Production of Recombinant Viruses by Use of a Large Culture Vessel with Active Gassing

TAKASHI OKADA,[1] TATSUYA NOMOTO,[1] TORU YOSHIOKA,[1] MUTSUKO NONAKA-SARUKAWA,[1] TAKAYUKI ITO,[1] TSUYOSHI OGURA,[1] MAYUMI IWATA-OKADA,[2] RYOSUKE UCHIBORI,[1] KUNIKO SHIMAZAKI,[3] HIROAKI MIZUKAMI,[1] AKIHIRO KUME,[1] and KEIYA OZAWA[1,2]

ABSTRACT

Adenovirus and adeno-associated virus (AAV) vectors are increasingly used for gene transduction experiments. However, to produce a sufficient amount of these vectors for *in vivo* experiments requires large-capacity tissue culture facilities, which may not be practical in limited laboratory space. We describe here a large-scale method to produce adenovirus and AAV vectors with an active gassing system that uses large culture vessels to process labor- and cost-effective infection or transfection in a closed system. Development of this system was based on the infection or transfection of 293 cells on a large scale, using a large culture vessel with a surface area of 6320 cm^2. A minipump was connected to the gas inlet of the large vessel, which was placed inside the incubator, so that the incubator atmosphere was circulated through the vessel. When active gassing was employed, the productivity of the adenovirus and AAV vectors significantly increased. This vector production system was achieved by improved CO_2 and air exchange and maintenance of pH in the culture medium. Viral production with active gassing is particularly promising, as it can be used with existing incubators and the large culture vessel can readily be converted for use with the active gassing system.

OVERVIEW SUMMARY

Large-scale production of recombinant viruses, using a large culture vessel with active gassing, is superior to protocols using standard tissue culture plates or flasks because of the higher capacity for cell growth. Although a previous protocol for recombinant virus production in a large culture vessel had the problem of insufficient transduction efficiency resulting from inadequate gas exchange, a method to use active gassing successfully improved productivity of recombinant viruses. Development of a vector production system on a large scale, using commercially available large culture vessels, allows us to process labor- and cost-effective manipulation in a closed system.

INTRODUCTION

ADENOVIRUS AND ADENO-ASSOCIATED VIRUS (AAV) VECTORS are highly efficient for transduction in many gene therapy studies (Okada *et al.*, 2002b, 2004; Ito *et al.*, 2003; Nomoto *et al.*, 2003; Yamaguchi *et al.*, 2003; Mochizuki *et al.*, 2004; Yoshioka *et al.*, 2004; Liu *et al.*, 2005). However, current production methods rely on the manipulation of many individual flasks and are not generally considered appropriate for scaling-up of production because it would be a time-consuming and labor-intensive process. Therefore, alternative tissue culture vessels with higher capacity for cell growth, such as a 10-tray Cell Factory (CF10; Nalge Nunc International, Rochester, NY) with a surface area of 6320 cm^2, could be suitable for scaling-up of

[1]Division of Genetic Therapeutics, Center for Molecular Medicine, Jichi Medical School, Tochigi 329-0498, Japan.
[2]Division of Hematology, Department of Medicine, Jichi Medical School, Tochigi 329-0498, Japan.
[3]Department of Physiology, Jichi Medical School, Tochigi 329-0498, Japan.

vector production (Okada *et al.*, 2002a). This device is easy to handle and can be used for efficient cell culture on a large scale in a closed system requiring only an air filter (Berger *et al.*, 2002; Tuyaerts *et al.*, 2002). Nevertheless, a previous protocol for recombinant virus production in the CF10 had the problem of insufficient scaling-up of vector production (Liu *et al.*, 2003). In that protocol, inadequate gas exchange between the culture vessel and the incubator might have been the cause of the inefficient yield.

We consequently adapted an active gassing system to generate large numbers of recombinant viruses in the CF10. The purpose of this active gassing is to control and maintain CO_2 tension and pH in the growth medium by passing a gas mixture through the CF10. For many types of cells, pH is an important parameter for controlling cell growth. This can be achieved by gassing with CO_2 in atmospheric air in the incubator. Enhanced gas exchange in a large culture vessel should improve both viral infectivity and plasmid transfection efficiency. In combination with the previously described method of using the CF10 (Okada *et al.*, 2002a), we have now created a simple and highly efficient system of producing vector stock on a large scale. Presented here is a labor- and cost-effective method for large-scale production of adenovirus and AAV vectors with an active gassing system that uses a large culture vessel to achieve transfection or infection in a closed system.

MATERIALS AND METHODS

Cell culture with active gassing

Propagation of vectors was based on the infection or transfection of human embryonic kidney-derived 293B cells (Yamaguchi *et al.*, 2003) by using either a flask with a surface area of 225 cm^2 (Falcon, T-225; BD Biosciences Discovery Labware, Bedford, MA) or the CF10, as described previously (Okada *et al.*, 2002a). Cells were cultured in Dulbecco's modified Eagle's medium and nutrient mixture F12 (DMEM–F12: Invitrogen, Grand Island, NY) with 10% fetal bovine serum (FBS; Sigma-Aldrich, St. Louis, MO), penicillin (100 units/ml), and streptomycin (100 μg/ml) at 37°C in a 5% CO_2 incubator. First, cells were plated at 2.3×10^6 cells per T-225 or at 6.5×10^7 cells per CF10 to achieve a monolayer at 20 to 40% confluency when cells initially attach to the surface of the flask. The volume of medium used per flask was 40 ml per T-225 or 1120 ml per CF10. Subsequently, cells were grown to a confluency of 70–90% over the next 48 to 72 hr for adenovirus infection or plasmid transfection. An aquarium pump (NISSO, Tokyo, Japan) was used to circulate air through the CF10 with 5% CO_2 and humidity control by an incubator. The CF10 was mounted with a bacterial air filter (bacterial air vents; Pall Gelman Sciences, Ann Arbor, MI) to connect the aquarium pump. The pump was connected to the gas inlet of the CF10 and the CF10 was placed inside the incubator, so that the incubator atmosphere was circulated through the CF10. The flow through the CF10 was maintained at 500 ml/min. Culture medium was sampled periodically, and the CO_2 concentrations and pH were estimated with a blood gas analyzer (Nova PHOX; Diamond Diagnostics, Holliston, MA). Glucose levels of the culture medium were also estimated with a glucose meter (Glutest Sensor, Glutest Ace GT-1640; Sanwa Kagaku Kenkyusho, Nagoya, Japan).

Construction and propagation of adenoviral vectors

A recombinant adenoviral vector, Ad-EGFP, was constructed using an adenoviral DNA–protein complex without a transgene insert (AVC2.null) (Okada *et al.*, 1998); it carried the cytomegalovirus (CMV) promoter, cloning sites, a simian virus 40 (SV40) intron, and the SV40 polyadenylation signal. To generate Ad-EGFP encoding enhanced green fluorescent protein (EGFP), a *Spe*I–*Cla*I fragment containing the *EGFP* cDNA excised from pEGFP-1 (BD Biosciences Clontech, Palo Alto, CA) was inserted into the *Xba*I and *Nsp*V sites in the DNA–protein complex, AVC2.null, using the direct *in vitro* ligation technique (Okada *et al.*, 1998). The ligated DNA–protein complex was introduced into 293 cells by the calcium phosphate transfection method. Viral plaques on 293 cells were isolated, amplified, and titrated by standard techniques. To amplify the vector in 293 cells, half the medium in the tissue culture flasks was exchanged with fresh DMEM–F12 containing 10% FBS 1 hr before infection. Cells were infected with the virus at 10 multiplicities of infection (MOI) per cell. Cells were incubated to reach full cytopathic effect, and crude viral lysate was purified by two rounds of CsCl two-tier centrifugation. The average number of plaque-forming units (PFU) was assessed on the basis of the 50% tissue culture infective dose. The number of vector particles was estimated by dot-blot hybridization of DNase I-treated stocks with plasmid standards.

Construction and propagation of AAV vectors

AAV1-EGFP, a recombinant AAV type 1 expressing the *EGFP* gene under the control of the CAG promoter (modified chicken β-actin promoter) with the CMV-IE enhancer, was generated by the following procedure. A *Bam*HI–*Xba*I fragment containing EGFP cDNA excised from pEGFP-1 and a *Hin*dIII fragment containing the woodchuck hepatitis virus posttranscriptional regulatory element (WPRE) sequence excised from pBluescript II SK(+)WPRE-B11 (a gift from T. Hope, University of Illinois at Chicago, Chicago, IL) was cloned into an *Xho*I site of pCAGGS (a gift from J.-i. Miyazaki, Osaka University Graduate School of Medicine, Japan) to create pCAG-EGFP-WPRE, using an *Xho*I linker. The EGFP expression cassette in pCAG-EGFP-WPRE was ligated to *Not*I-excised pAAV-LacZ to form the proviral vector plasmid pAAV2-CAG-EGFP-WPRE. AAV viral stocks were prepared according to a previously described protocol (Okada *et al.*, 2002a) with minor modifications. Half the medium in tissue culture flasks was exchanged with fresh DMEM–F12 containing 10% FBS 1 hr before plasmid transfection. Subsequently, cells were cotransfected with 23 μg (per T-225) or 650 μg (per CF10) of each of the following plasmids: a proviral vector plasmid, AAV-1 chimeric helper plasmid p1RepCap (Mochizuki *et al.*, 2004), and adenoviral helper plasmid pAdeno, by a calcium phosphate coprecipitation method. Each of the vector and helper plasmids was added to 4 ml (per T-225) or 112 ml (per CF10) of 300 m*M* $CaCl_2$. This solution was gently added to an equal volume of 2× HEPES-buffered saline (HBS: 290 m*M* NaCl, 50 m*M* HEPES buffer, 1.5 m*M* Na_2HPO_4, pH 7.0) and immediately mixed by gentle inversion three times to form a uniform solution. This solution was immediately mixed with fresh DMEM–F12 containing 10% FBS outside the flasks to produce a homogeneous plasmid solution mixture. Subsequently, medium in the

culture flasks was entirely replaced with this plasmid solution mixture. At the end of incubation for 6 hr, the plasmid solution mixture in the culture flasks was replaced with prewarmed fresh DMEM–F12 containing 2% FBS. Cell suspensions were collected 72 hr after transfection and centrifuged at 300 × *g* for 10 min. Each cell pellet was resuspended in 2 ml (per T-225) or 56 ml (per CF10) of Tris-buffered saline (TBS: 100 m*M* Tris-HCl [pH 8.0], 150 m*M* NaCl). Recombinant AAV was harvested by three cycles of freeze–thawing of each resuspended pellet. Crude viral lysate was then purified twice by passage through a CsCl two-tier centrifugation gradient, as described previously (Okada *et al.*, 2002b). The viral stock was titrated by dot-blot hybridization of DNase I-treated stocks with plasmid standards. To confirm transgene expression with the propagated vector *in vivo*, 5-week-old male Sprague-Dawley rats were injected via the anterior tibial muscle with AAV1-EGFP (1×10^{11} genome copies per rat). Fifteen weeks after injection, the rats were sacrificed and expression was confirmed by fluorescence microscopy.

Statistical analysis

Statistical significance was determined on the basis of an unpaired, two-tailed p value and Student t test, and a p value less than 0.05 was considered significant.

RESULTS

Improved gas exchange and maintenance of pH in medium after recombinant adenovirus infection

Propagation of vectors was based on infection or transfection of 293 cells on a large scale. A minipump was connected to the gas inlet of the CF10 and placed inside the incubator, so that the atmosphere in the incubator, containing 5% CO_2, was circulated through the CF10. The gas flow for circulation through the CF10 was maintained at 500 ml/min. An appropriate gas flow rate was important to give a uniform distribution of the gas in the individual trays of the CF10. A flow less than 200 ml/min gave uneven distribution of the gas, and significantly influenced cell growth. Gas flow that was too high also disturbed the uniformity of cell density. Appropriate cell density and uniform distribution of cells are critical to achieve successful gene transduction. Application of active gassing significantly increased cell growth in the CF10 (Table 1). CO_2 concentrations in the media stayed at their initial levels when using either a T-225 or CF10 with active gassing (Fig. 1A). In contrast, the CO_2 concentration inside the CF10 increased subsequent to adenovirus infection in the absence of active gassing. The pH of culture medium in the CF10 with active gassing was close to that in the T-225 and significantly higher than that in the CF10 without active gassing (Fig. 1B).

Monitoring of cell numbers and time point for harvest

The glucose level was monitored as an index for tracing cell growth and cytopathic effect in the CF10 to avoid the necessity for a specialized microscope to monitor cells in the large culture vessel. The glucose level decreased with increasing cell confluency and progression of cytopathic effect (CPE) (Fig. 2). When 80% CPE was reached, the glucose level was reduced to about 50 mg/ml. When glucose levels were less than 25%, the cells showed full CPE and this was regarded as the appropriate time for harvest.

Improved adenovirus vector production in a large culture vessel with active gassing

We estimated the adenovirus vector yield propagated by using 28 T-225 flasks with a surface area of 225 cm^2, a CF10 with a surface area of 6320 cm^2, or a CF10 in the presence of active gassing. When active gassing was used with the CF10, the productivity of the adenovirus vectors was dramatically increased, by 53.4 times compared with that in the CF10 without active gassing (Fig. 3). The vector yield per producer cell in the CF10 was also significantly improved in the presence of active gassing (Table 1). The PFU-to-particle ratios for vectors produced in the T-225, CF10, and CF10 with active gassing were 1:7, 1:15, and 1:10, respectively.

Efficient AAV vector production in a large culture vessel with active gassing

Enhanced gas exchange in a large culture vessel should also improve vector production through plasmid transfection. AAV vectors were produced in a large vessel by a three-plasmid transfection adenovirus-free protocol (Okada *et al.*, 2002b). Three days after plasmid transfection, the CO_2 concentrations in medium from the CF10 in the presence of active gassing were significantly less than those without active gassing (Table 2). The pH of the culture medium in the CF10 with active gassing was also improved. The CF-10 with active gassing was compatible with the three-plasmid transfection protocol for recombinant AAV production. When we used active gassing, the vec-

TABLE 1. INCREASED CELL GROWTH AND VECTOR YIELD WITH ACTIVE CO_2 AND AIR EXCHANGE[a]

Flask	*Number of cells harvested*	*Vector yield per cell (PFU/cell)*
225-cm^2 flask	$(1.4 \pm 0.2) \times 10^9$ (per 28 flasks)	7.9×10^3
CF10	$(4.9 \pm 1.6) \times 10^8$	4.1×10^2
CF10 + AG	$(1.3 \pm 0.3) \times 10^9$	8.2×10^3

[a]At the time of cell harvest after adenovirus infection, cell growth and vector yield per cell in a CF10 with a surface area of 6320 cm^2 in the presence or absence of active gassing (AG) were compared with that in 28 flasks with a surface area of 225 cm^2 each.

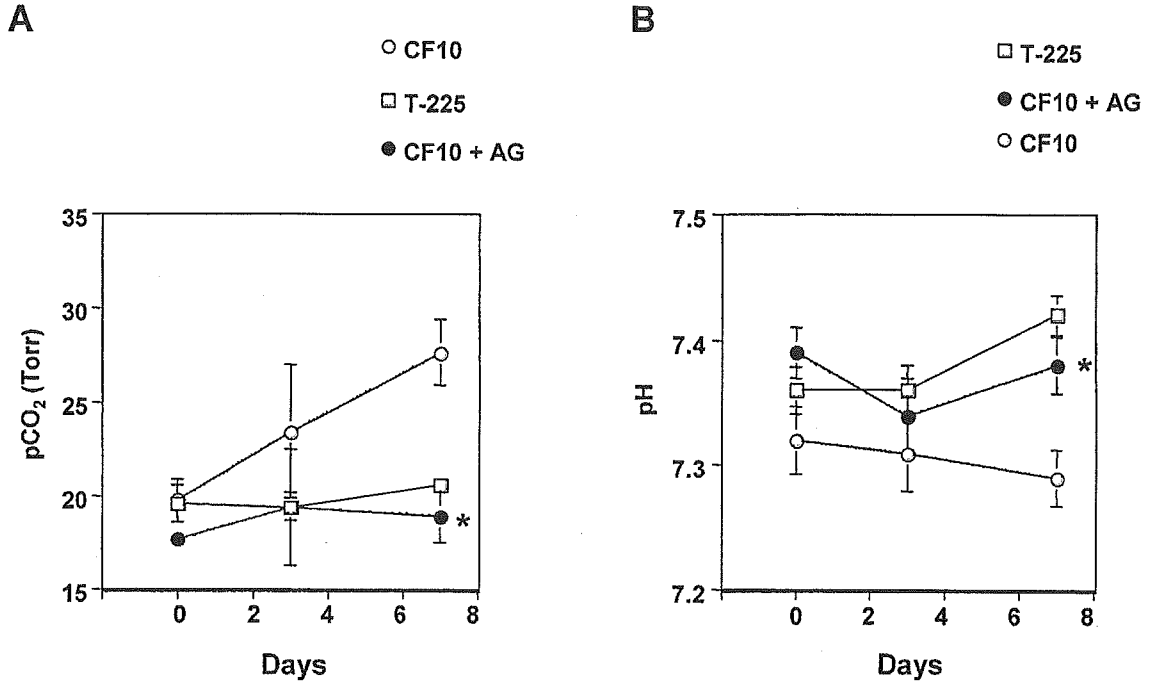

FIG. 1. Improved CO_2 and air exchange and maintenance of pH in conditioned medium after recombinant adenovirus infection. Subsequent to adenovirus infection in a normal flask with a surface area of 225 cm^2 (T-225) or a large culture vessel (a 10-tray Cell Factory [CF10] with a surface area of 6320 cm^2) in the presence or absence of active gassing (AG), CO_2 concentrations (**A**) and pH (**B**) in conditioned medium were determined ($n = 4$). Asterisk indicates $p < 0.05$ in comparison with a CF10 without AG.

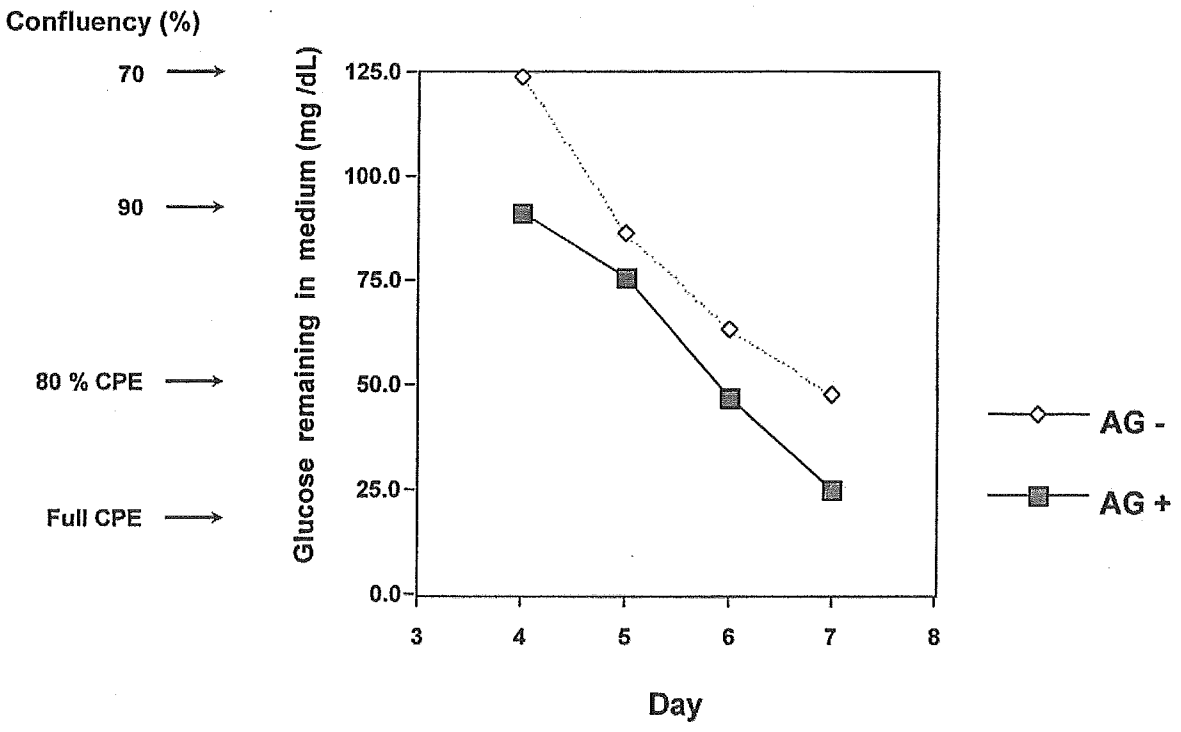

FIG. 2. Glucose reading to monitor cell growth. Glucose reading of culture medium was used as an index to monitor cell growth and cytopathic effect (CPE) in the CF10 to avoid the need for a specialized microscope. Cells were infected with recombinant adenovirus in the presence or absence of active gassing (AG) when 90% confluent.

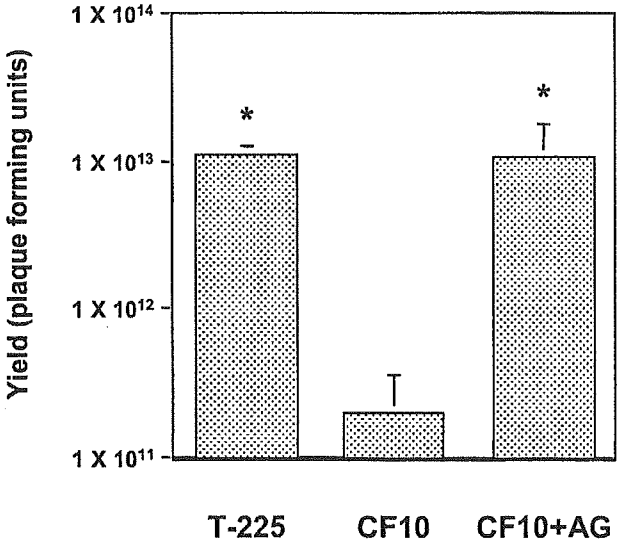

FIG. 3. Improved production of adenovirus vector. Adenovirus vector was propagated in 28 T-225 flasks ($n = 4$), a CF10 ($n = 3$), or a CF10 in the presence of active gassing (CF10 + AG, $n = 3$). Adenovirus vector expressing an EGFP reporter gene was generated in two independent experiments. The average number of plaque-forming units (PFU) was assessed by $TCID_{50}$. *$p < 0.05$ in comparison with a CF10 without AG.

TABLE 2. ENHANCED GAS EXCHANGE AND MAINTENANCE OF pH IN CONDITIONED MEDIUM AFTER PLASMID TRANSFECTION[a]

	pCO_2 (Torr)	*pH*
CF10	25.6 ± 1.1	7.23 ± 0.03
CF10 + AG	14.2 ± 0.1	7.40 ± 0.01

[a]Three days after plasmid transfection by using CF10 in the presence or absence of active gassing (AG), CO_2 concentrations and pH in the conditioned medium were estimated. Means ± standard deviations are shown ($n = 4$).

TABLE 3. IMPROVED YIELDS OF RECOMBINANT AAV TYPE 1 BY ACTIVE GAS EXCHANGE[a]

	Yield per vessel	*Yield per cell*
CF10	$(2.2 \pm 0.5) \times 10^{12}$	$(3.1 \pm 0.6) \times 10^{3}$
CF10 ± AG	$(1.0 \pm 0.7) \times 10^{13}$	$(1.1 \pm 0.7) \times 10^{4}$

[a]Titers of AAV1-EGFP were determined as genome copies by dot-blot analysis of DNase-treated stocks. AG, active gassing. Means ± standard deviations are shown ($n = 4$).

tor yield per cell was increased significantly, by 3.5 times (Table 3). Although vector yield was dependent on the transgene and construct, production of vector particles at up to 2.0×10^{13} genome copies per CF-10 was achieved.

Transduction of muscles with AAV vectors produced in a large culture vessel with active gassing

Five-week-old male Sprague-Dawley rats were injected with AAV1-enhanced green fluorescence protein (EGFP) (1×10^{11} genome copies per rat) via the anterior tibial muscle. Fifteen weeks after injection, the rats were sacrificed to confirm expression by fluorescence microscopy. The injected sites showed efficient expression of EGFP (Fig. 4).

DISCUSSION

Successful vector production in a large culture vessel was achieved by improvement of CO_2 and air exchange along with maintenance of pH in the medium. Adenovirus production was enhanced by more than 50 times with the active gassing sys-

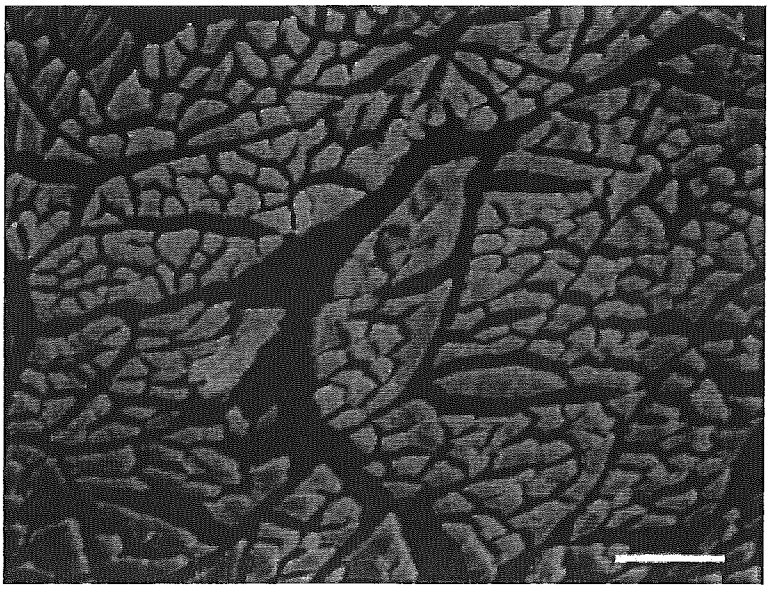

FIG. 4. Transduction of muscles with AAV vectors *in vivo*. Five-week-old male Sprague-Dawley rats were injected with AAV1-EGFP (1×10^{11} genome copies per body) via the anterior tibial muscle. Fifteen weeks after injection, the rats were killed to confirm expression by fluorescence microscopy. Scale bar: 100 μm.

tem. CF-10 with active gassing was also compatible with the three-plasmid transfection protocol for recombinant AAV production. When we used active gassing, the productivity of the AAV vectors was significantly increased.

In a direct comparison with vectors generated in ordinary culture flasks, viruses from the CF10 with active gassing were equivalent regarding function and bioactivity. The use of a CF10 with active gassing thus resulted in the production of vectors equivalent to those obtained in conventional culture dishes, but with a dramatically reduced workload. An average yield of approximately 1.0×10^{13} PFU requires as many as 28 T-225 flasks, according to our previous protocol. Alternatively, only one CF10 with active gassing was enough to achieve the same amount of virus. Furthermore, the PFU-to-particle ratio was also increased with the use of active gassing, suggesting improved bioactivity of the viruses. We used this system to amplify various adenovirus vectors. Although vector yield was dependent on the transgene and construct, a proportional increase in yield relative to surface area was achieved (data not shown).

The system was also compatible with plasmid transfection for recombinant AAV production. Active gassing combined with a large culture vessel significantly increased the productivity of the AAV vectors. The effect of enhanced gas exchange on the productivity of AAV vectors was less than the effect on the productivity of adenovirus vectors. Because lactate production accompanied by adenovirus replication is much greater than that with AAV, the protection of cells against pH drop by maintaining the CO_2 tension might be a plausible explanation for the preferential effect on adenovirus production. Transient transfection in a large culture vessel also provides a simple and flexible method of producing lentivirus-based vectors (Karolewski *et al.*, 2003). Therefore, our protocol would also be applicable to the efficient production of lentivirus- or retrovirus-based vectors.

Because this system fits into existing incubators and current vessels can readily be converted to the active gassing system, the viral production protocol using a CF-10 coupled with active gassing has practical utility for growing recombinant virus stocks in a limited laboratory space. This system has proven successful in our repeated manipulations and appears particularly promising. We have used the CF10 with the active gassing system in more than 400 vector preparations in the course of our more recent gene therapy experiments. The system allows us to perform a considerable number of *in vivo* experiments and to validate our studies.

ACKNOWLEDGMENTS

The authors thank Dr. Villy Nielsen, Ph.D. (Nunc, Roskilde, Denmark) and Mr. Hiroyuki Sano (Nalge Nunc International, Japan) for helpful discussions. We thank Avigen (Alameda, CA) for providing pAAV-LacZ and pAdeno. We thank Dr. Thomas Hope (University of Illinois at Chicago) for providing pBluescript II SK(+)WPRE-B11 and Dr. Jun-ichi Miyazaki (Osaka University Graduate School of Medicine, Japan) for pCAGGS. We also thank Ms. Miyoko Mitsu and Mr. Masataka Takahashi (Ieda Chemicals, Japan) for their encouragement and technical support. This study was supported in part by grants from the Ministry of Health, Labor, and Welfare of Japan; Grants-in-Aid for Scientific Research; a grant for the 21st Century Center of Excellence Program; and a matching fund subsidy from the High-Tech Research Center Project for Private Universities, through the Ministry of Education, Culture, Sports, Science, and Technology of Japan.

REFERENCES

BERGER, T.G., FEUERSTEIN, B., STRASSER, E., HIRSCH, U., SCHREINER, D., SCHULER, G., and SCHULER-THURNER, B. (2002). Large-scale generation of mature monocyte-derived dendritic cells for clinical application in cell factories. J. Immunol. Methods **268,** 131–140.

ITO, A., OKADA, T., MIZUGUCHI, H., HAYAKAWA, T., MIZUKAMI, H., KUME, A., TAKATOKU, M., KOMATSU, N., HANAZONO, Y., and OZAWA, K. (2003). A soluble CAR–SCF fusion protein improves adenoviral vector-mediated gene transfer to c-Kit-positive hematopoietic cells. J. Gene Med. **5,** 929–940.

KAROLEWSKI, B.A., WATSON, D.J., PARENTE, M.K., and WOLFE, J.H. (2003). Comparison of transfection conditions for a lentivirus vector produced in large volumes. Hum. Gene Ther. **14,** 1287–1296.

LIU, Y., OKADA, T., SHEYKHOLESLAMI, K., SHIMAZAKI, K., NOMOTO, T., MURAMATSU, S., KANAZAWA, T., TAKEUCHI, K., AJALLI, R., MIZUKAMI, H., KUME, A., ICHIMURA, K., and OZAWA, K. (2005). Specific and efficient transduction of cochlear inner hair cells with recombinant adeno-associated virus type 3 vector. Mol. Ther. (in press).

LIU, Y.L., WAGNER, K., ROBINSON, N., SABATINO, D., MARGARITIS, P., XIAO, W., and HERZOG, R.W. (2003). Optimized production of high-titer recombinant adeno-associated virus in roller bottles. Biotechniques **34,** 184–189.

MOCHIZUKI, S., MIZUKAMI, H., KUME, A., MURAMATSU, S., TAKEUCHI, K., MATSUSHITA, T., OKADA, T., KOBAYASHI, E., HOSHIKA, A., and OZAWA, K. (2004). Adeno-associated virus (AAV) vector-mediated liver- and muscle-directed transgene expression using various kinds of promoters and serotypes. Gene Ther. Mol. Biol. **8,** 9–18.

NOMOTO, T., OKADA, T., SHIMAZAKI, K., MIZUKAMI, H., MATSUSHITA, T., HANAZONO, Y., KUME, A., KATSURA, K., KATAYAMA, Y., and OZAWA, K. (2003). Distinct patterns of gene transfer to gerbil hippocampus with recombinant adeno-associated virus type 2 and 5. Neurosci. Lett. **340,** 153–157.

OKADA, T., RAMSEY, W.J., MUNIR, J., WILDNER, O., and BLAESE, R.M. (1998). Efficient directional cloning of recombinant adenovirus vectors using DNA–protein complex. Nucleic Acids Res. **26,** 1947–1950.

OKADA, T., NOMOTO, T., SHIMAZAKI, K., LIJUN, W., LU, Y., MATSUSHITA, T., MIZUKAMI, H., URABE, M., HANAZONO, Y., KUME, A., MURAMATSU, S., NAKANO, I., and OZAWA, K. (2002a). Adeno-associated virus vectors for gene transfer to the brain. Methods **28,** 237–247.

OKADA, T., SHIMAZAKI, K., NOMOTO, T., MATSUSHITA, T., MIZUKAMI, H., URABE, M., HANAZONO, Y., KUME, A., TOBITA, K., OZAWA, K., and KAWAI, N. (2002b). Adeno-associated viral vector-mediated gene therapy of ischemia-induced neuronal death. Methods Enzymol. **346,** 378–393.

OKADA, T., CAPLEN, N.J., RAMSEY, W.J., ONODERA, M., SHIMAZAKI, K., NOMOTO, T., AJALLI, R., WILDNER, O., MORRIS, J., KUME, A., HAMADA, H., BLAESE, R.M., and OZAWA, K. (2004). *In situ* generation of pseudotyped retroviral progeny by adenovirus-mediated transduction of tumor cells enhances the killing effect of HSV-tk suicide gene therapy *in vitro* and *in vivo*. J. Gene Med. **6,** 288–299.

TUYAERTS, S., NOPPE, S.M., CORTHALS, J., BRECKPOT, K., HEIRMAN, C., DE GREEF, C., VAN RIET, I., and THIELEMANS,

K. (2002). Generation of large numbers of dendritic cells in a closed system using Cell Factories. J. Immunol. Methods **264,** 135–151.

YAMAGUCHI, T., OKADA, T., TAKEUCHI, K., TONDA, T., OHTAKI, M., SHINODA, S., MASUZAWA, T., OZAWA, K., and INABA, T. (2003). Enhancement of thymidine kinase-mediated killing of malignant glioma by BimS, a BH3-only cell death activator. Gene Ther. **10,** 375–385.

YOSHIOKA, T., OKADA, T., MAEDA, Y., IKEDA, U., SHIMPO, M., NOMOTO, T., TAKEUCHI, K., NONAKA-SARUKAWA, M., ITO, T., TAKAHASHI, M., MATSUSHITA, T., MIZUKAMI, H., HANAZONO, Y., KUME, A., OOKAWARA, S., KAWANO, M., ISHIBASHI, S., SHIMADA, K., and OZAWA, K. (2004). Adeno-associated virus vector-mediated interleukin-10 gene transfer inhibits atherosclerosis in apolipoprotein E-deficient mice. Gene Ther. **11,** 1772–1779.

Address reprint requests to:
Dr. Takashi Okada
Division of Genetic Therapeutics
Center for Molecular Medicine
Jichi Medical School
3311-1 Yakushiji
Minami-Kawachi, Tochigi 329-0498, Japan

E-mail: tokada@jichi.ac.jp

Received for publication May 17, 2005; accepted after revision August 8, 2005.

Published online: September 21, 2005.

doi:10.1016/j.ymthe.2005.03.021

ARTICLE

Specific and Efficient Transduction of *Cochlear* Inner Hair Cells with Recombinant Adeno-associated Virus Type 3 Vector

Yuhe Liu,[1,2] Takashi Okada,[1] Kianoush Sheykholeslami,[3] Kuniko Shimazaki,[4] Tatsuya Nomoto,[1] Shin-Ichi Muramatsu,[5] Takeharu Kanazawa,[6] Koichi Takeuchi,[7] Rahim Ajalli,[2] Hiroaki Mizukami,[1] Akihiro Kume,[1] Keiichi Ichimura,[2] and Keiya Ozawa[1,*]

[1]*Division of Genetic Therapeutics, Center for Molecular Medicine, Jichi Medical School, 3311-1 Yakushiji, Minami-kawachi, Kawachi, Tochigi 329-0498, Japan*
[2]*Department of Otolaryngology and Head and Neck Surgery, Jichi Medical School, 3311-1 Yakushiji, Minami-kawachi, Kawachi, Tochigi 329-0498, Japan*
[3]*Department of Neurobiology, Northeastern Ohio Universities College of Medicine, Rootstown, OH 44272, USA*
[4]*Department of Physiology, Jichi Medical School, 3311-1 Yakushiji, Minami-kawachi, Kawachi, Tochigi 329-0498, Japan*
[5]*Department of Medicine, Division of Neurology, Jichi Medical School, 3311-1 Yakushiji, Minami-kawachi, Kawachi, Tochigi 329-0498, Japan*
[6]*Department of Otolaryngology and Head and Neck Surgery, Faculty of Medicine, University of the Ryukyus, Okinawa 903-0213, Japan*
[7]*Department of Anatomy, Jichi Medical School, 3311-1 Yakushiji, Minami-kawachi, Kawachi, Tochigi 329-0498, Japan*

**To whom correspondence and reprint requests should be addressed. Fax: (+81) 285 44 8675. E-mail: kozawa@jichi.ac.jp.*

Available online 12 May 2005

Recombinant adeno-associated virus (AAV) vectors are of interest for cochlear gene therapy because of their ability to mediate the efficient transfer and long-term stable expression of therapeutic genes in a wide variety of postmitotic tissues with minimal vector-related cytotoxicity. In the present study, seven AAV serotypes (AAV1–5, 7, 8) were used to construct vectors. The expression of EGFP by the chicken β-actin promoter associated with the cytomegalovirus immediate-early enhancer in cochlear cells showed that each of these serotypes successfully targets distinct cochlear cell types. In contrast to the other serotypes, the AAV3 vector specifically transduced cochlear inner hair cells with high efficiency *in vivo*, while the AAV1, 2, 5, 7, and 8 vectors also transduced these and other cell types, including spiral ganglion and spiral ligament cells. There was no loss of cochlear function with respect to evoked auditory brain-stem responses over the range of frequencies tested after the injection of AAV vectors. These findings are of value for further molecular studies of cochlear inner hair cells and for gene replacement strategies to correct recessive genetic hearing loss due to monogenic mutations in these cells.

Key Words: adeno-associated virus, serotype, gene transfer, cochlea, hair cells

INTRODUCTION

The total number of hair cells in the cochlea is finite. They are not renewed and there is very little (if any) redundancy in this population. The irreversible loss of cochlear hair cells is presumed to be a fundamental cause of permanent sensorineural hearing loss. Gene transfer into hair cells presents numerous opportunities for protecting these cells. There is considerable interest in the development of viral vectors to deliver genes to the cochlea to counteract hearing impairment, and recent studies have focused on vectors based on adenovirus [1–3], herpes simplex virus [4–6], lentivirus [7], and adeno-associated virus (AAV) [8,9]. The patterns of vector-encoded transgene expression have been found to differ significantly among vectors. Cochlear hair cells can be efficiently transduced with adenovirus vectors [10–12]. However, these vectors were found to provoke a strong immune response that could damage recipient cells and compromise cochlear function [10,13,14]; they are also incapable of mediating prolonged transgene expression [15,16]. Although AAV vectors might overcome these problems, the transduction of hair cells by AAV2-derived vectors is controversial [8,10,17]. To our knowledge, other AAV serotypes have not yet been tested as cochlear gene transfer vectors *in vitro* or *in vivo*. AAV vectors are of interest in the context of gene therapy because they mediate efficient transfer and long-term stable expression of therapeutic genes in a wide variety of postmitotic tissues with minimal vector-related cytotoxicity.

In this study, we assessed the utility of seven AAV serotypes as vectors with the chicken β-actin promoter associated with a cytomegalovirus immediate-early

1525-0016/$30.00

doi:10.1016/j.ymthe.2005.03.021

enhancer (CAG)-driven enhanced green fluorescent protein (EGFP) gene [18] in the murine cochlea. Vectors were introduced by microinjection through the round window membrane [19]. As a result, we determined that the specific and efficient gene transduction of inner hair cells could be achieved by using AAV type 3 vectors.

RESULTS

Expression Profile of EGFP in the Cochlea

Several cell types line the cochlear duct and support the hair cells (Fig. 1A). We carefully made a small opening in the tympanic bulla and injected vectors derived from the AAV1–4, 7, and 8 pseudotypes into the cochlea of two strains of mice (C57BL/6J and ICR) through the round window membrane (Fig. 1B). The mode of EGFP expression in various murine cochlear hair cells had a close similarity and was essentially equal for both strains. We determined the distribution of AAV vector-mediated EGFP expression throughout the cochlea for all serotypes tested (Table 1). A principal finding is that the inner hair cells in the organ of Corti showed clear evidence of EGFP expression with all of the AAV serotype-derived vectors except for the AAV4 vector (Fig. 2). This result indicates that most of the vectors (AAV1–5, 7, and 8) could efficiently transduce cochlear inner hair cells *in vivo* when slowly infused into the scala tympani. The AAV3-based vector was the most efficient and specific of the serotypes in transducing cochlear inner hair cells (Fig. 3). Transduction with 5×10^{10} genome copies (gc)/cochlea of the AAV3 vector resulted in robust transgene expression in the inner hair cells. The spiral ganglion cells showed significantly higher levels of fluorescence per unit area with the AAV5-based vector (Fig. 2n), and the spiral ligament cells were transduced prominently with the AAV1 and AAV7 vectors (Figs. 2d and 2r). Histological sections of cochleae injected with the AAV4 vector identified EGFP-positive cells predominantly in connective tissue within the mesothelial cells beneath the organ of Corti and in mesenchymal cells lining the perilymphatic fluid spaces (Figs. 2j and 2l). Furthermore, we detected intense expression with the AAV5- and AAV8-based vectors in the inner sulcus cells and in Claudius' cells (Figs. 2p and 2x). We did not detect notable levels of gene expression in the outer hair cells, supporting pillar cells, or stria vascularis cells for any serotype.

Long-term Expression of EGFP

We examined cochlear expression of the EGFP transgene in animals sacrificed at 1–12 weeks. Expression persisted in cochlear tissues for up to 3 months after infusion, while the extent of expression peaked at 2 weeks.

Transgene Activity

We determined the percentage of inner hair cells transduced with the AAV3 vector. The mid- to high-frequency regions of the cochlea were efficiently transduced, as shown in Fig. 3. Almost all of the inner hair cells in the basal and middle cochlear regions were transduced with the AAV3 vector (Fig. 4). Transgene expression was not detected in the hair cells of the apical turn of the cochlea. The predominant expression in the middle and basal cochlear turns is reasonable, as the virus

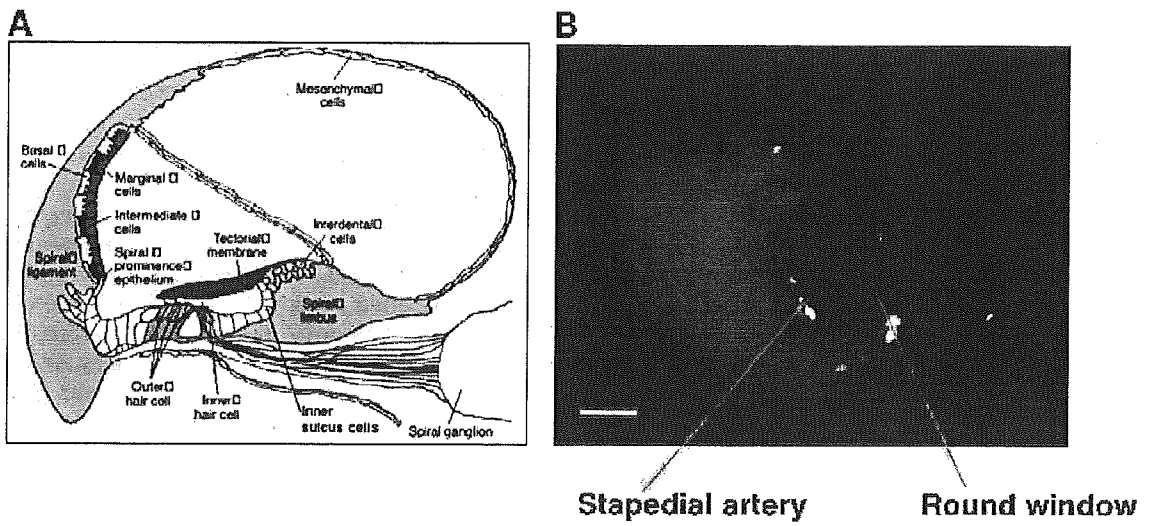

FIG. 1. (A) Schematic diagram of a cross section of the cochlea, demonstrating the scala vestibuli, scala tympani, and scala media or cochlear duct. The organ of Corti rests on the basilar membrane, with the hair cell cilia embedded in the gelatinous tectorial membrane. The outer margin of the cochlear duct contains the stria vascularis. Reproduced, by permission of the publisher, from [44]. (B) Direct visualization of the round window membrane in the right ear. The upper side of the picture is the back of the mouse and the right side is the head of the animal. The stapedial artery, a branch of the internal carotid artery, transverses an open bony semicanal within the round window niche. Bar denotes 500 μm, 15× original magnification.

TABLE 1: Expression of transgene in the mouse cochlea with vectors derived from the AAV1–4, 7, and 8 pseudotypes

Vector	Inner hair cells	Outer hair cells	Spiral ganglion	Stria vascularis	Spiral ligament	Spiral limbus	Reissner's membrane	Inner and outer pillar cells	Inner sulcus cells	Deiter's cells	Claudius' cells	Hensen's cells	Mesenchymal cells
AAV1	+++	–	++	–	++	++	++	–	+	–	–	–	++
AAV2	++	–	+	–	+	+	–	–	–	–	–	–	–
AAV3	+++	–	–	–	–	–	–	–	–	–	–	–	–
AAV4	–	–	–	–	–	–	–	–	–	–	–	–	+
AAV5	+++	–	+++	–	+	++	+	–	++	–	+	–	–
AAV7	+++	–	+	–	+++	++	–	–	+	–	+	–	++
AAV8	+++	–	–	–	+	+	–	–	++	–	+	–	+

The level of expression was graded by fluorescence intensity on a four-level scale (+, ++, +++, ++++) depending on the pixel/unit area count. ++++ means the strongest intensity of EGFP expression, + means the weakest intensity of EGFP expression, while – means no fluorescence.

was slowly infused into the scala tympani adjacent to the most basal turn of the cochlea. The percentage of transduced inner hair cells from the basal (high frequencies) to the apical (low frequencies) cochlear regions is shown in Fig. 4.

Cytotoxicity

We detected no deleterious effects on the viability of transduced cells. We compared evoked auditory brainstem response (ABR) threshold levels before and after injection, using a two-way repeated measure of the analysis of variance. There was no significant loss in ABR and hence no change in cochlear function for up to 10 days following vector infusion (Figs. 5A and 5B). In addition, the cellular and tissue architecture of experimental cochleae remained intact. There was no evidence of endolymphatic hydrops after AAV vector injection in any of the animals. We observed no significant destruction of the inner or outer hair cells (Fig. 5C).

Discussion

In the present study, we assessed the utility of vectors derived from seven AAV serotypes for gene delivery into the cochlea. Our results showed that the AAV3 vector was the most efficient and specific in transducing cochlear inner hair cells, although these cells could also be transduced with AAV1, 2, 5, 7, and 8 vectors. The transduction efficiency of the spiral ganglion by the AAV5 vector was particularly high, followed by that of the AAV1, AAV2, and AAV7 vectors. The efficient and specific transduction of inner hair cells with the AAV3 vector suggests that it recognizes a unique host range with a distinct cellular receptor. Transduction efficiency is dependent on initial viral binding (a property of the viral capsid), entry, and various postentry processes such as intracellular trafficking and second-strand synthesis [20–22]. The genome size of AAV vectors has also been demonstrated to affect transduction efficiency [23]. Comparisons of the serotypes have indicated that heterogeneity in the capsid-encoding regions and a differential ability to transduce cells may be associated with different receptor and co-receptor requirements for cell entry [24]. However, the receptors and co-receptors of AAV3 have not yet been clearly identified.

In the current study, we found that cochlear inner hair cells could be transduced with six AAV serotypes, although Lalwini *et al.* [8] reported that outer hair cells could be transduced with a low titer (1×10^6 viral particles/ml) of AAV2 *in vivo*. After injecting the AAV2 vector, we found that the spiral ganglion neurons, the inner hair cells, and the cells in the spiral ligament were all transduced. This transduction pattern differs from that reported in previous studies [8,10,17], and this discrepancy might be due to the different delivery methods and dissimilar promoters. Although the CAG promoter directs

doi:10.1016/j.ymthe.2005.03.021

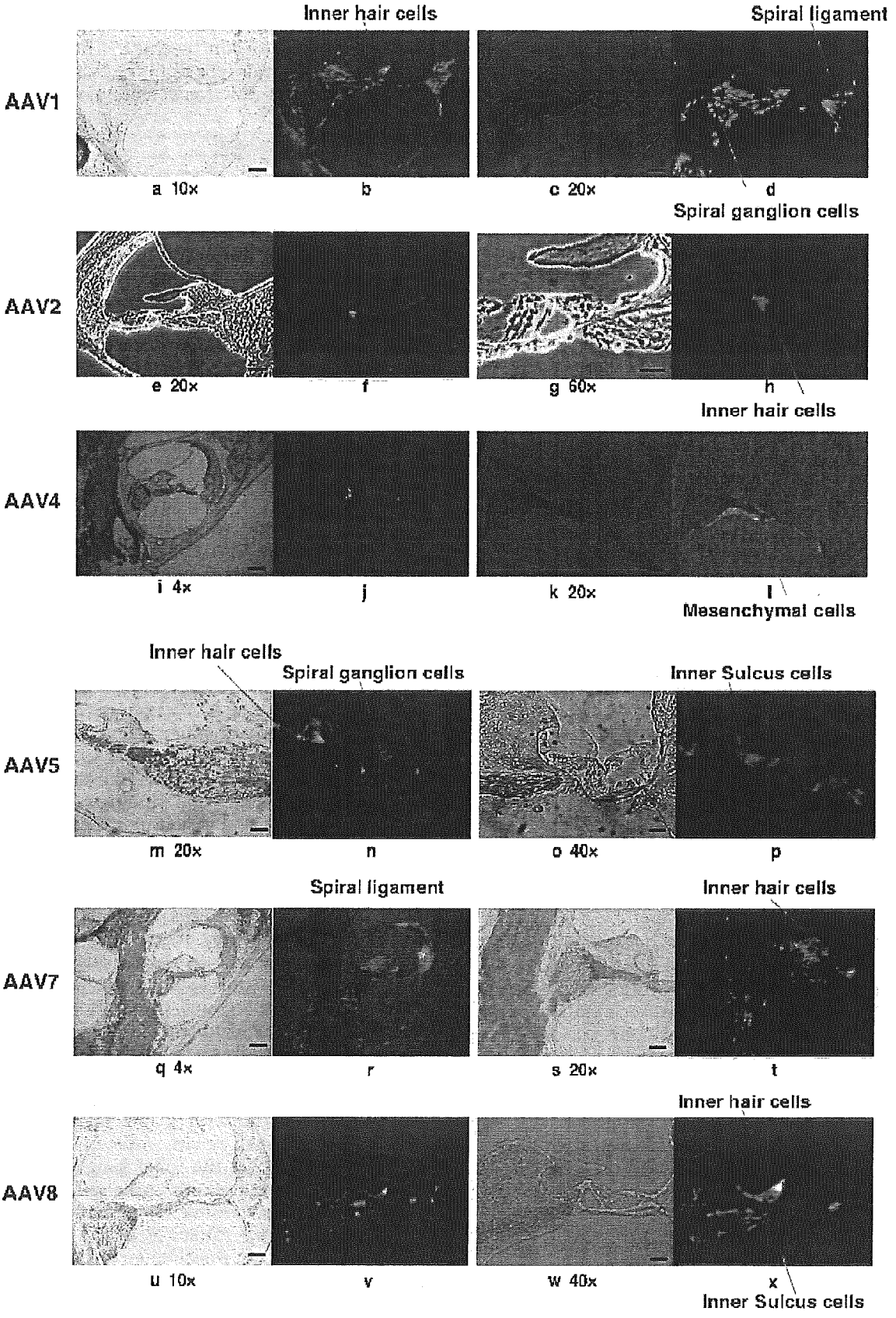

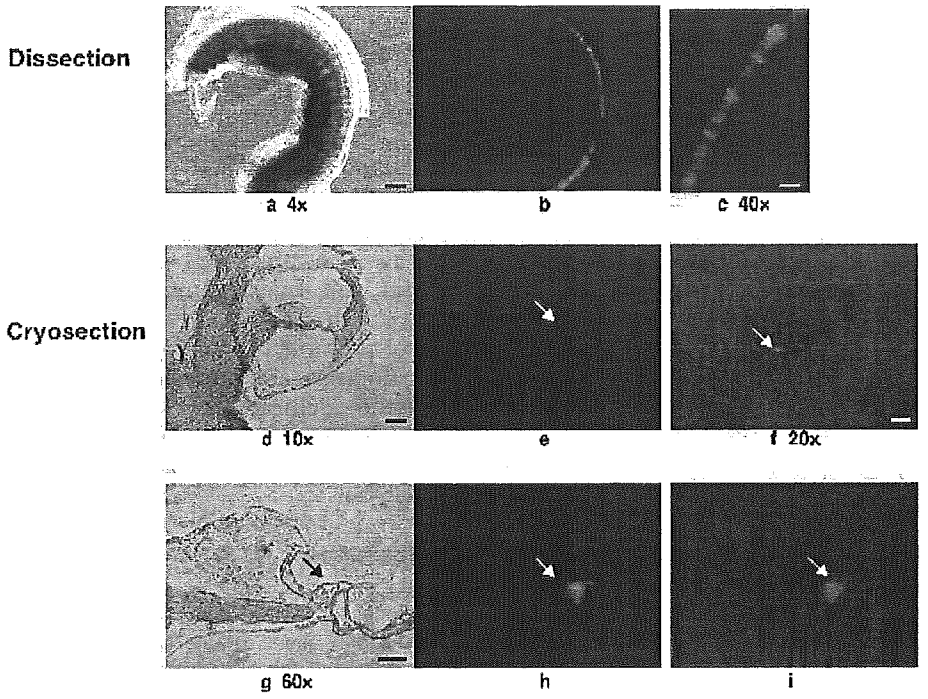

FIG. 3. Cochlear transduction with AAV3-CAG-EGFP. Dissected cochleae and cryosections show transgene expression in inner hair cells. (a) A light photomicrograph of the basal turn of the cochlea is shown, illustrating its laminar structure. (b) A fluorescence photomicrograph of this dissection. (c) A higher magnification view of the dissection shown in (b), illustrating a row of inner hair cells in the organ of Corti expressing EGFP. (d–i) Representative photomicrographs from three magnifications of a radial cochlear cryosection. (d) Light photomicrography of an intact cochlear duct. Fluorescence photomicrography of this duct is shown in (e). (h and i) A higher magnification of (e), illustrating EGFP expression within inner hair cells. Cryosections show transgene expression in the inner hair cells (arrows). Scale bars: 4×, 250 μm; 10×, 100 μm; 20×, 50 μm; 40×, 25 μm; 60×, 25 μm.

higher expression than do the cytomegalovirus (CMV) and EF-1α promoters [25], each promoter drives reporter gene expression in different cell types [26,27].

Cell-specific or -selective infectivity of the viral vectors suggests the presence of various factors to introduce the distinct expression patterns of the transgenes. Spiral ganglion neurons and glial cells can be transduced with a lentivirus–GFP construct *in vitro* but not *in vivo* [7]. The differential transducibility under *in vivo* and *in vitro* conditions reflects a high degree of structural isolation of the spiral ganglion and other cell types—such as the cells on the periphery of the endolymph—from the perilymph into which the viral vector was introduced. The strict separation of the endolymph from the perilymph is maintained by tight junctions that line the boundary between these fluid chambers. The size of the viral particle may contribute to the observed variability in transgene expression promoted by different vectors. The diameters of adenovirus and retrovirus (including lentivirus) particles are approximately 75 nm and greater than 100 nm, respectively, while the diameters of AAV vectors are typically 11–22 nm [28,29]. Thus, the larger size of lentiviruses and adenoviruses may limit their subsequent dissemination from the perilymph into the endolymph. The variable patterns of adenovirus- and lentivirus-mediated gene expression seen with different methods of inoculation may be due to the inoculation route, the volume and number of viral particles, differences in viral preparation, or differences in the method of transgene detection. The introduction of adenovirus vectors by cochleostomy or with an osmotic pump via the round window leads to a more efficient transduction of cochlear hair cells [30–32]. The apical domain (apical membrane and stereocilia) of cells in the sensory epithelium (hair cells and supporting cells) is bathed in endolymph, while the basal–lateral domain is immersed in perilymph. Access of the viral vectors to the endolymphatic space by cochleostomy may facilitate the transduction of hair cells and supporting cells. However, although the cochleostomy procedure has been tested, inoculation into the membranous labyrinth could not be confirmed [32]. In the present study, AAV vectors were found to infect cochlear hair cells easily *in vivo,* via round window injection.

Gene transfer into the cochlea through the round window membrane is ideal, because this procedure

FIG. 2. Transduction of the cochleae by AAV1-, AAV2-, AAV4-, AAV5-, AAV7-, and AAV8-based vectors. (a, c, e, g, i, k, m, o, q, s, u, and w) Light photomicrographs of cochlear cryosections. (b, d, f, h, j, l, n, p, r, t, v, and x) Fluorescence photomicrographs (green fluorescence from transgene). The spiral ligament cells were transduced prominently with the AAV1 and AAV7 vectors (d and r). Transgene expression in inner hair cells was detected with AAV1-, AAV2-, AAV5-, AAV7-, and AAV8-based vectors (b, h, n, t, and x). AAV4-based vector faintly transduced mesenchymal cells (j and l). The spiral ganglion cells showed significant levels of fluorescence with the AAV5-based vector (n). Intense fluorescence was detected with the AAV5- and AAV8-based vectors in the inner sulcus cells (p and x). Scale bars: 10×, 100 μm; 20×, 50 μm; 40×, 25 μm; 60×, 25 μm.

doi:10.1016/j.ymthe.2005.03.021

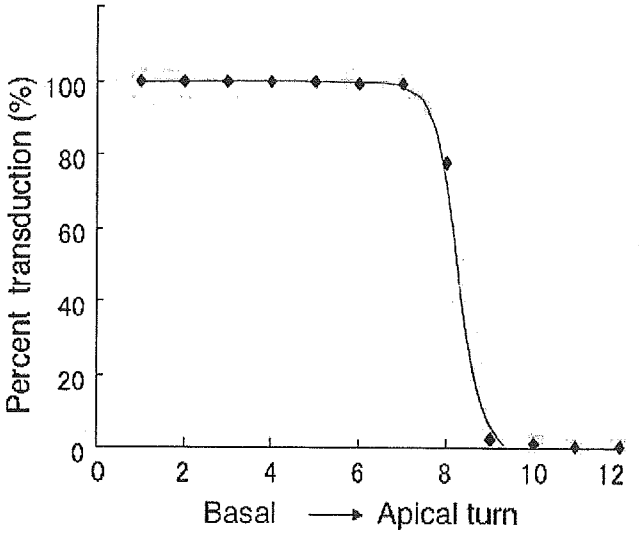

FIG. 4. EGFP expression profile of inner hair cells transduced with AAV3, as shown for a cross section subdivided into 12 segments ranging from the basal (high frequencies) to the apical (low frequencies) cochlear regions.

requires simple surgery without cochlear trauma [19]. Another critical factor in assessing the utility of a gene transfer vector is safety. Factors determining safety include the toxicity of the gene transfer agent itself, the provocation of immune responses, the generation of replication-competent virus, and the risk of creating genetically modified cells by insertional mutagenesis. The cells and tissues within the AAV-EGFP-perfused cochleae were free from inflammation and were generally intact. No pathological changes were observed in the organ of Corti, stria vascularis, or spiral ganglion cells. The long-term expression of EGFP within the cochlear tissues is consistent with data obtained from other animal models and different organ systems [9,33]. Since EGFP is known to introduce cellular toxicity, vectors expressing physiologically therapeutic proteins would achieve longer transduction periods than EGFP. Gene transfer into the inner hair cells presents numerous opportunities for auditory neuroscience. Potential applications include the localization of proteins by expression of tagged constructs, the generation of dominant-negative or antisense knockouts of endogenous proteins, the rescue of mutant phenotypes to identify disease genes, and perhaps even the treatment of auditory disorders. Advances in the molecular basis of auditory diseases have allowed the identification of a number of genetic disorders such as presbycusis, acoustic trauma, and ototoxicity. The development of gene therapy now allows us to evaluate the effects of transferring therapeutic genes into the inner ear by several different strategies. The expression of marker genes in the inner ear tissue has been demonstrated. Further studies will improve our understanding of cochlear function as well as provide for the development of novel therapies for a wide variety of inner ear diseases. Intracochlear gene transfer using AAV vectors has been established as a viable experimental proposition. Future study will include the transfer of functioning genes *in vivo* and the development of alternative vectors. While clinical application may be some way off, it is vital that gene delivery techniques are optimized in anticipation of future need.

In conclusion, the data presented in this paper demonstrate successful gene transfer into several types of cochlear cells *in vivo* with AAV-based vectors. Interestingly, the AAV3 vector promoted inner hair cell-specific transduction. These findings are of value for further molecular studies of the cochlear inner hair cells and for gene replacement strategies to correct hereditary hearing loss due to specific monogenic mutations affecting cochlear inner hair cells.

MATERIALS AND METHODS

Construction and preparation of proviral plasmids. The AAV vector proviral plasmid pAAV2-*LacZ* harbors an *Escherichia coli* β-galactosidase expression cassette with the CMV promoter, the first intron of the human growth hormone gene, and the SV40 early polyadenylation sequence, which are flanked by inverted terminal repeats (ITRs) [34]. The *LacZ* expression cassette of pAAV2-*LacZ* was ligated to *Not*I-excised pAAV5-RNL [35] to form the proviral plasmid pAAV5-*LacZ*. The pAAV2-CAG-EGFP-WPRE construct consists of the EGFP gene under the control of the CAG promoter (the chicken β-actin promoter associated with the cytomegalovirus immediate-early enhancer) and WPRE (woodchuck hepatitis virus posttranscriptional regulatory element) flanked by ITRs. The WPRE cassette augments the stability of transgene mRNA [36] and increases EGFP expression levels, thereby ensuring long-term transgene expression. A *Bam*HI–*Xba*I fragment containing the EGFP cDNA excised from pEGFP-1 and a *Hin*dIII fragment containing the WPRE sequence excised from pBS II SK$^+$WPRE-B11 (a gift from Dr. J. Donello) was ligated to *Xho*I linkers and cloned into an *Xho*I site of pCAGGS (a gift from Dr. J.-I. Miyazaki) to create pCAG-EGFP-WPRE. The EGFP expression cassette from pCAG-EGFP-WPRE was ligated to the *Not*I-excised pAAV2-*LacZ* and pAAV5-RNL [35] to form the proviral plasmids pAAV2-CAG-EGFP-WPRE and pAAV5-CAG-EGFP-WPRE, respectively. The AAV-helper plasmid harbors Rep and Cap. The adenovirus helper plasmid pAdeno5 (identical to pVAE2AE4-5) encodes the entire E2A and E4 regions and the VA RNA I and II genes [37]. Plasmids were purified with the Qiagen plasmid purification kits (Qiagen K.K., Tokyo, Japan).

Recombinant AAV vector production. Vectors derived from the AAV1–4, 7, and 8 pseudotypes were produced with the AAV packaging plasmid pAAV1RepCap (for AAV1) [38], pHLP19 (for AAV2), pAAV3RepCap (for AAV3) [39], pAAV4RepCap (for AAV4) [40], pAAV7RepCap (for AAV7) [41], or pAAV8RepCap (for AAV8) [41] and the AAV proviral plasmid pAAV2-*LacZ* or pAAV2-CAG-EGFP-WPRE. The plasmids pAAV5RepCap [35] and pAAV5-*LacZ*, or pAAV5-CAG-EGFP-WPRE, were used to produce vector with the AAV5 pseudotype [42]. Seven AAV serotype vectors were produced as previously described by the three-plasmid transfection adenovirus-free protocol [37]. Briefly, three days before transfection, 293 cells were plated onto a 10-tray Cell Factory (Nalge Nunc International, Rochester, NY, USA; 6×10^7 cells/10-tray). The cells were cotransfected with 650 μg each of the proviral plasmid, the AAV vector packaging plasmid, and the adenovirus helper plasmid pAdeno5 [34] by the calcium phosphate coprecipitation method. The medium was changed following incubation for 6–8 h at 37°C. Recombinant AAV was harvested 72 h after transfection by three freeze/thaw cycles. The crude viral lysate was purified twice on a cesium chloride two-tier centrifugation

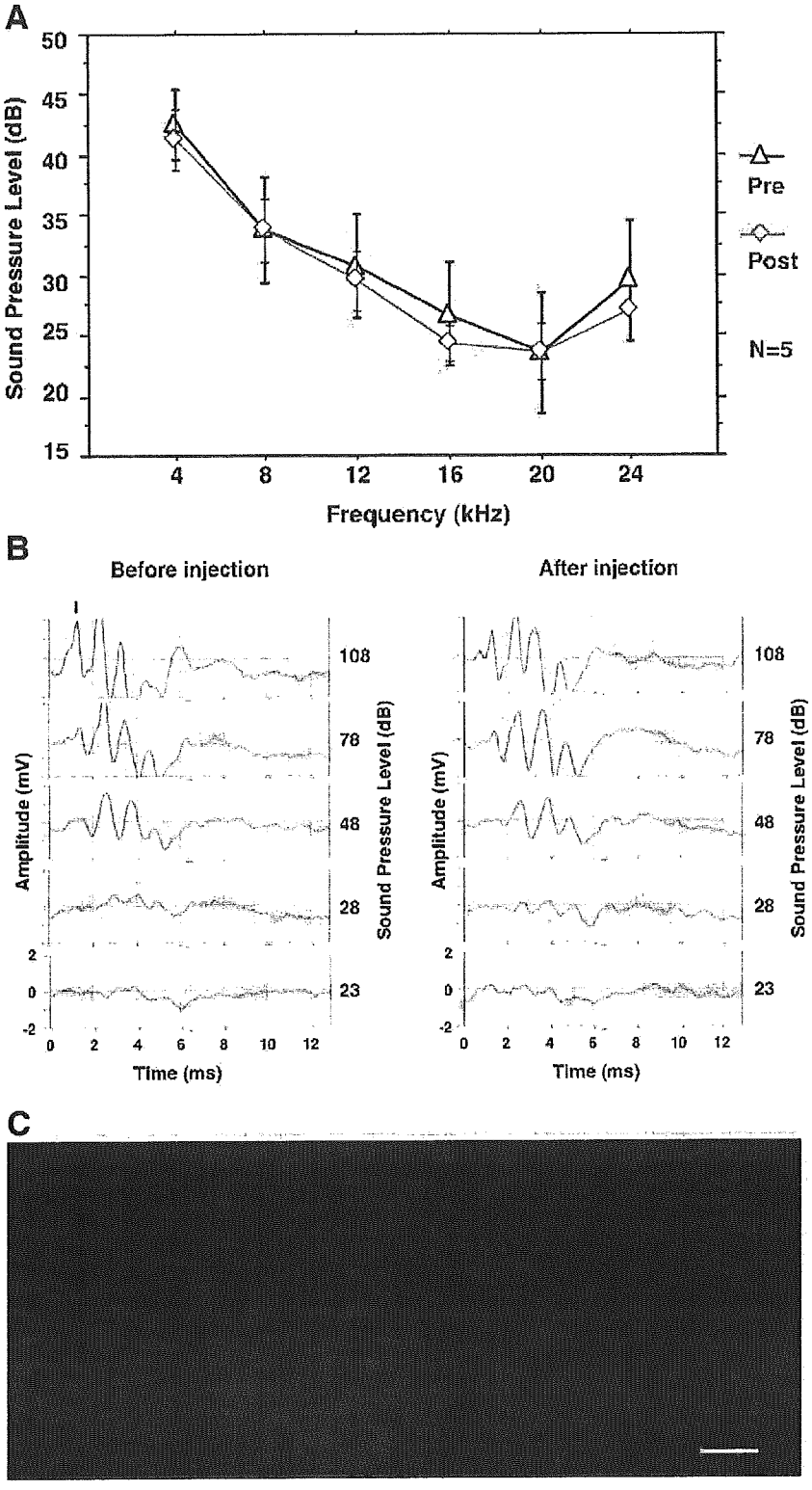

FIG. 5. (A) ABR threshold (mean ± SD) at each frequency tested preoperatively (pre) versus postoperatively (post). (B) Example of ABR waveforms in C57BL/6J at various stimuli (16 kHz; 108 dB, 78 dB, 48 dB, 28 dB, and 23 dB). ABR were tested in the transduced ear prior to viral injection and 10 days after injection. Wave I was measured to analyze the activity of the cochlea. (C) F-actin staining showing that no outer hair cells were lost from inoculated cochleae. Original magnification 40×; scale bar, 25 μm.

gradient as described previously [24]. The viral stock was treated with DNase and titrated by quantitative real-time PCR with plasmid standards [43].

Surgical procedures and cochlear perfusions. All animal studies were performed in accordance with the guidelines issued by the committee on animal research of Jichi Medical School and approved by its ethics

doi:10.1016/j.ymthe.2005.03.021

committee. Sixty female C57BL/6J mice (4 weeks of age; CLEA Japan, Tokyo, Japan) and 40 male ICR mice (2 months of age; Japan SLC, Shizuoka, Japan) were utilized. The mice were initially anesthetized with ketamine (50 mg/kg) and the analgesic xylazine (5 mg/kg). A postauricular approach was used to expose the tympanic bony bulla. A small opening (2 mm) in the tympanic bulla was carefully made to allow access to the round window membrane. In the tested groups, 5 μl AAV vector solution (5×10^{10} gc) was microinjected into the cochlea through the round window over 10 min with a glass micropipette (40 μm in diameter) fitted on a Univentor 801 syringe pump (Serial No. 170182, High Precision Instruments, Univentor Ltd., Malta) [19]. A small plug of muscle was used to seal the cochlea and the surgical wound was closed in layers and dressed with antibiotic ointment. Five mice of each strain received control cochlear perfusions with artificial perilymph (145 mM NaCl, 2.7 mM KCl, 2 mM $MgSO_4$, 1.2 mM $CaCl_2$, 5 mM Hepes) alone. Each AAV-EGFP serotype was injected into five mice of each strain. Another 20 C57BL/6J mice were injected with the AAV3 vector to study long-term expression.

Cochlear function assessment using ABR. To assess the physiological status of experimental ears, auditory thresholds were determined with multiple frequency and intensity tone bursts by performing ABR audiometry with Tucker–Davis Technologies and Scope v3.6.9 software (Power Lab/200; ADInstruments, Castle Hill, Australia). Tone pipes were introduced into the operated ears of the anesthetized mice, and evoked potentials were recorded using needle electrodes inserted through the skin. ABR were elicited and measured 256 times at 4, 8, 12, 16, 20, and 24 kHz frequencies with tone bursts in systematic 5-dB steps. The rise/fall times for the tone bursts were 0.1 ms rise/ms flat (cosine gate). Free-field system was used as a calibration procedure. Wave I was measured to analyze the activity from the cochlea. The lowest stimulus level that yielded a detectable ABR waveform was defined as the threshold. ABR were tested in the infused ear prior to surgery and 10 days postsurgery. Data were statistically analyzed using repeated-measures analysis of variance followed by paired Student's t test performed with StatView 5.0 software (SAS Institute Inc., Cary, NC, USA). Values of $P < 0.05$ were considered significant.

Histology. Cochlear transgene expression patterns were determined for all AAV serotypes by visualizing EGFP expression. The animals were sacrificed 10 days after injection, and intracardiac perfusion was performed with 4% paraformaldehyde (PFA) in 0.1 M phosphate buffer, pH 7.4. The cochleae were harvested and the stapes footplates were removed. For AAV3-mediated transduction, the animals (five mice for each time point) were sacrificed 1, 2, 4, 8, or 12 weeks after inoculation. Postfixation was carried out in 4% PFA for 4 h at 4°C, and decalcification was performed in 10% EDTA for 12 days at room temperature. The cochlear half-turns were microdissected and processed and the other half-turns were prepared by cryosection (10 μm) to detect EGFP expression by using an Olympus IX70 (Olympus Corp., Tokyo, Japan) fluorescence microscope with a standard fluorescein isothiocyanate filter set and Studio Lite software (Olympus Corp.). Cells that exhibited fluorescence were considered positive for transgene expression. The level of expression was graded by fluorescence intensity on a four-point scale (+, ++, +++, ++++) depending on the pixel/unit area count. Hair cell counts were carried out with dissected cochlea.

ACKNOWLEDGMENTS

The authors thank Avigen, Inc. (Alameda, CA, USA) for providing pAAV-LacZ, pHLP19, and pAdeno; Dr. John A. Chiorini for pAAV4RepCap (identical to pSV40oriAAV4-2), pAAV5-RNL, and pAAV5RepCap (identical to 5RepCapB); and Dr. James M. Wilson for pAAV7RepCap and pAAV8RepCap. We also thank Dr. John E. Donello (Infectious Disease Laboratory, The Salk Institute for Biological Studies) for providing pBS II SK+WPRE-B11 and Dr. Jun-Ichi Miyazaki (Osaka University Graduate School of Medicine) for pCAGGS. The authors also thank Mr. Takeshi Hayakawa (Bio Research Center Co., Ltd.), Ms. Miyoko Mitsu, and Ms. Kiyomi Aoki for their encouragement and technical support. This study was supported in part by (1) grants from the Ministry of Health, Labor, and Welfare of Japan; (2) Grants-in-Aid for Scientific Research; (3) a grant from the 21 Century COE Program; and (4) the High-Tech Research Center Project for Private Universities matching fund subsidy from the Ministry of Education, Culture, Sports, Science, and Technology of Japan.

RECEIVED FOR PUBLICATION NOVEMBER 1, 2004; ACCEPTED MARCH 24, 2005.

REFERENCES

1. Raphael, Y., Frisancho, J. C., and Roessler, B. J. (1996). Adenoviral-mediated gene transfer into guinea pig cochlear cells in vivo. *Neurosci. Lett.* **207:** 137–141.
2. Holt, J. R., *et al.* (1999). Functional expression of exogenous proteins in mammalian sensory hair cells infected with adenoviral vectors. *J. Neurophysiol.* **81:** 1881–1888.
3. Yamasoba, T., Suzuki, M., and Kondo, K. (2002). Transgene expression in mature guinea pig cochlear cells in vitro. *Neurosci. Lett.* **335:** 13–16.
4. Derby, M. L., Sena-Esteves, M., Breakefield, X. O., and Corey, D. P. (1999). Gene transfer into the mammalian inner ear using HSV-1 and vaccinia virus vectors. *Hear. Res.* **134:** 1–8.
5. Chen, X., Frisina, R. D., Bowers, W. J., Frisina, D. R., and Federoff, H. J. (2001). HSV amplicon-mediated neurotrophin-3 expression protects murine spiral ganglion neurons from cisplatin-induced damage. *Mol. Ther.* **3:** 958–963.
6. Bowers, W. J., Chen, X., Guo, H., Frisina, D. R., Federoff, H. J., and Frisina, R. D. (2002). Neurotrophin-3 transduction attenuates cisplatin spiral ganglion neuron ototoxicity in the cochlea. *Mol. Ther.* **6:** 12–18.
7. Han, J. J., *et al.* (1999). Transgene expression in the guinea pig cochlea mediated by a lentivirus-derived gene transfer vector. *Hum. Gene Ther.* **10:** 1867–1873.
8. Lalwani, A. K., Walsh, B. J., Reilly, P. G., Muzyczka, N., and Mhatre, A. N. (1996). Development of in vivo gene therapy for hearing disorders: introduction of adeno-associated virus into the cochlea of the guinea pig. *Gene Ther.* **3:** 588–592.
9. Lalwani, A., *et al.* (1998). Long-term in vivo cochlear transgene expression mediated by recombinant adeno-associated virus. *Gene Ther.* **5:** 277–281.
10. Luebke, A. E., Foster, P. K., Muller, C. D., and Peel, A. L. (2001). Cochlear function and transgene expression in the guinea pig cochlea, using adenovirus- and adeno-associated virus-directed gene transfer. *Hum. Gene Ther.* **12:** 773–781.
11. Luebke, A. E., Steiger, J. D., Hodges, B. L., and Amalfitano, A. (2001). A modified adenovirus can transfect cochlear hair cells in vivo without compromising cochlear function. *Gene Ther.* **8:** 789–794.
12. Staecker, H., Li, D., O'Malley, B. W., Jr., and Van De Water, T. R. (2001). Gene expression in the mammalian cochlea: a study of multiple vector systems. *Acta Otolaryngol.* **121:** 157–163.
13. Dazert, S., Aletsee, C., Brors, D., Gravel, C., Sendtner, M., and Ryan, A. (2001). In vivo adenoviral transduction of the neonatal rat cochlea and middle ear. *Hear. Res.* **151:** 30–40.
14. Ishimoto, S., Kawamoto, K., Kanzaki, S., and Raphael, Y. (2002). Gene transfer into supporting cells of the organ of Corti. *Hear. Res.* **173:** 187–197.
15. Van de Water, T. R., Staecker, H., Halterman, M. W., and Federoff, H. J. (1999). Gene therapy in the inner ear: mechanisms and clinical implications. *Ann. N.Y. Acad. Sci.* **884:** 345–360.
16. Vassalli, G., Bueler, H., Dudler, J., von Segesser, L. K., and Kappenberger, L. (2003). Adeno-associated virus (AAV) vectors achieve prolonged transgene expression in mouse myocardium and arteries in vivo: a comparative study with adenovirus vectors. *Int. J. Cardiol.* **90:** 229–238.
17. Li Duan, M., Bordet, T., Mezzina, M., Kahn, A., and Ulfendahl, M. (2002). Adenoviral and adeno-associated viral vector mediated gene transfer in the guinea pig cochlea. *Neuroreport* **13:** 1295–1299.
18. Lalwani, A. K., Han, J. J., Walsh, B. J., Zolotukhin, S., Muzyczka, N., and Mhatre, A. N. (1997). Green fluorescent protein as a reporter for gene transfer studies in the cochlea. *Hear. Res.* **114:** 139–147.
19. Kho, S. T., Pettis, R. M., Mhatre, A. N., and Lalwani, A. K. (2000). Cochlear microinjection and its effects upon auditory function in the guinea pig. *Eur. Arch. Otorhinolaryngol.* **257:** 469–472.
20. Handa, A., Muramatsu, S., Qiu, J., Mizukami, H., and Brown, K. E. (2000). Adeno-associated virus (AAV)-3-based vectors transduce haematopoietic cells not susceptible to transduction with AAV-2-based vectors. *J. Gen. Virol.* **81:** 2077–2084.
21. Davidson, B. L., *et al.* (2000). Recombinant adeno-associated virus type 2, 4, and 5 vectors: transduction of variant cell types and regions in the mammalian central nervous system. *Proc. Natl. Acad. Sci. USA* **97:** 3428–3432.
22. Zabner, J., *et al.* (2000). Adeno-associated virus type 5 (AAV5) but not AAV2 binds to the apical surfaces of airway epithelia and facilitates gene transfer. *J. Virol.* **74:** 3852–3858.
23. Yang, G. S., *et al.* (2002). Virus-mediated transduction of murine retina with adeno-associated virus: effects of viral capsid and genome size. *J. Virol.* **76:** 7651–7660.
24. Okada, T., *et al.* (2002). Adeno-associated virus vectors for gene transfer to the brain. *Methods* **28:** 237–247.
25. Xu, L., *et al.* (2001). CMV-beta-actin promoter directs higher expression from an

adeno-associated viral vector in the liver than the cytomegalovirus or elongation factor 1 alpha promoter and results in therapeutic levels of human factor X in mice. *Hum. Gene Ther.* **12:** 563–573.
26. Chung, S., Andersson, T., Sonntag, K. C., Bjorklund, L., Isacson, O., and Kim, K. S. (2002). Analysis of different promoter systems for efficient transgene expression in mouse embryonic stem cell lines. *Stem Cells* **20:** 139–145.
27. Nomoto, T., *et al.* (2003). Distinct patterns of gene transfer to gerbil hippocampus with recombinant adeno-associated virus type 2 and 5. *Neurosci. Lett.* **340:** 153–157.
28. Dutta, S. K. (1975). Isolation and characterization of an adenovirus and isolation of its adenovirus-associated virus in cell culture from foals with respiratory tract disease. *Am. J. Vet. Res.* **36:** 247–250.
29. Palmer, E., and Goldsmith, C. S. (1988). Ultrastructure of human retroviruses. *J. Electron Microsc. Tech.* **8:** 3–15.
30. Stover, T., Yagi, M., and Raphael, Y. (1999). Cochlear gene transfer: round window versus cochleostomy inoculation. *Hear. Res.* **136:** 124–130.
31. Stover, T., Yagi, M., and Raphael, Y. (2000). Transduction of the contralateral ear after adenovirus-mediated cochlear gene transfer: round window versus cochleostomy inoculation. *Gene Ther.* **7:** 377–383.
32. Kawamoto, K., Oh, S. H., Kanzaki, S., Brown, N., and Raphael, Y. (2001). The functional and structural outcome of inner ear gene transfer via the vestibular and cochlear fluids in mice. *Mol. Ther.* **4:** 575–585.
33. Kaplitt, M. G., *et al.* (1994). Long-term gene expression and phenotypic correction using adeno-associated virus vectors in the mammalian brain. *Nat. Genet.* **8:** 148–154.
34. Okada, T., *et al.* (2001). Development and characterization of an antisense-mediated prepackaging cell line for adeno-associated virus vector production. *Biochem. Biophys. Res. Commun.* **288:** 62–68.
35. Chiorini, J. A., Kim, F., Yang, L., and Kotin, R. M. (1999). Cloning and characterization of adeno-associated virus type 5. *J. Virol.* **73:** 1309–1319.
36. Zufferey, R., Donello, J. E., Trono, D., and Hope, T. J. (1999). Woodchuck hepatitis virus posttranscriptional regulatory element enhances expression of transgenes delivered by retroviral vectors. *J. Virol.* **73:** 2886–2892.
37. Matsushita, T., *et al.* (1998). Adeno-associated virus vectors can be efficiently produced without helper virus. *Gene Ther.* **5:** 938–945.
38. Mochizuki, S., *et al.* (2004). Adeno-associated virus (AAV) vector-mediated liver- and muscle-directed transgene expression using various kinds of promoters and serotypes. *Gene Ther. Mol. Biol.* **8:** 9–18.
39. Muramatsu, S., Mizukami, H., Young, N. S., and Brown, K. E. (1996). Nucleotide sequencing and generation of an infectious clone of adeno-associated virus 3. *Virology* **221:** 208–217.
40. Chiorini, J. A., Yang, L., Liu, Y., Safer, B., and Kotin, R. M. (1997). Cloning of adeno-associated virus type 4 (AAV4) and generation of recombinant AAV4 particles. *J. Virol.* **71:** 6823–6833.
41. Gao, G. P., Alvira, M. R., Wang, L., Calcedo, R., Johnston, J., and Wilson, J. M. (2002). Novel adeno-associated viruses from rhesus monkeys as vectors for human gene therapy. *Proc. Natl. Acad. Sci. USA* **99:** 11854–11859.
42. Rabinowitz, J. E., *et al.* (2002). Cross-packaging of a single adeno-associated virus (AAV) type 2 vector genome into multiple AAV serotypes enables transduction with broad specificity. *J. Virol.* **76:** 791–801.
43. Veldwijk, M. R., *et al.* (2002). Development and optimization of a real-time quantitative PCR-based method for the titration of AAV-2 vector stocks. *Mol. Ther.* **6:** 272–278.
44. Kikuchi, T., *et al.* (1995). *Anat. Embryol. (Berlin)* **191:** 101–118.

Frag1, a homolog of alternative replication factor C subunits, links replication stress surveillance with apoptosis

Hideshi Ishii*, Taeko Inageta*, Koshi Mimori†, Toshiyuki Saito‡, Hiroki Sasaki§, Masaharu Isobe¶, Masaki Mori†, Carlo M. Croce‖**, Kay Huebner‖, Keiya Ozawa*, and Yusuke Furukawa*

*Center for Molecular Medicine, Jichi Medical School, Tochigi 329-0498, Japan; †Institute of Bioregulation, Kyushu University, Ohita 874-0838, Japan; ‡Transcriptome Profiling Group, National Institute for Radiological Science, Chiba 263-8555, Japan; §Genetics Division, National Cancer Center Research Institute, Tokyo 104-0045, Japan; ¶Faculty of Engineering, Toyama University, Toyama 930-8555, Japan; and ‖Department of Molecular Virology, Immunology, and Medical Genetics, Comprehensive Cancer Center, Ohio State University, Columbus, OH 43210

Contributed by Carlo M. Croce, May 23, 2005

We report the identification and characterization of a potent regulator of genomic integrity, mouse and human *FRAG1* gene, a conserved homolog of replication factor C large subunit that is homologous to the alternative replication factor C subunits Elg1, Ctf18/Chl12, and Rad24 of budding yeast. *FRAG1* was identified in a search for key caretaker genes involved in the regulation of genomic stability under conditions of replicative stress. In response to stress, Atr participates in the down-regulation of *FRAG1* expression, leading to the induction of apoptosis through the release of Rad9 from damaged chromatin during the S phase of the cell cycle, allowing Rad9–Bcl2 association and induction of proapoptotic Bax protein. We propose that the Frag1 signal pathway, by linking replication stress surveillance with apoptosis induction, plays a central role in determining whether DNA damage is compatible with cell survival or whether it requires cell elimination by apoptosis.

genomic integrity | Bcl2 | Rad9 | Atr | Rb

Replicative stress causes replication fork stalling or arrest, which can occur in yeast at naturally occurring sequences, such as replication fork barriers and replication slow zones (1). When damage is severe or the natural order of DNA replication is perturbed, DNA double-strand breaks can occur (2). Such events can trigger cellular checkpoints, allowing time for repair of damage before cell cycle progression (2). When the breaks are fixed or the damage is compatible with cell survival, double-strand breaks can give rise to the fixed chromosomal aberrations observed in cancer cells, such as translocations, inversions, amplifications, and deletions. Accumulated aberrations of caretaker pathways in concert with alterations of gatekeeper tumor suppressors give rise to transformed cells that acquire selective growth and survival advantages (3). Thus, the pathology of stalled or collapsed replication forks is important for understanding the role of faithful regulation of replication in preventing carcinogenesis.

Genotoxic stress-induced replication stalling activates checkpoint-signaling pathways that block cell cycle progression, control DNA repair, or trigger apoptosis (4) through membrane death receptors and the endogenous mitochondrial death pathways (5). Rad9 protein is involved in the control of the DNA damage-induced checkpoint (6). Studies in yeast and human cells have shown that Rad9 interacts with Hus1 and Rad1 in the 9-1-1 complex, which is a heterotrimeric complex and acts as a proliferating cell nuclear antigen-like sliding clamp (4, 7). In response to DNA damage, the 9-1-1 complex is loaded around DNA lesions by Rad17, which binds to chromatin before damage (8) and facilitates Atr-mediated phosphorylation and activation of Chk1 kinase to arrest cell cycle. Rad9 can participate in signaling apoptosis by interacting with antiapoptotic Bcl-2 family proteins Bcl-2 and Bcl-X_L but not with proapoptotic Bax and Bad (9). The interaction of Bcl2 with Bax prevents Bax from inducing cytochrome *c* release and cell death, and the Bax/Bcl2 ratio is crucial for regulation of apoptosis (10). Because the 9-1-1 clamp is also involved in DNA repair (7), the Rad9 complex is thought to play a key role in coordinating multiple functions of checkpoint activation, DNA repair, and apoptosis.

In this study, we report the identification and characterization of the *FRAG1* gene, which encodes a 1,820-aa mouse and 1,844-aa human conserved, uncharacterized protein homolog of the large replication factor C (RFC) subunit Rfc1 (861 aa) and the alternative RFC subunits Elg1 (791 aa), Ctf18/Chl12 (741 aa), and Rad24 (659 aa; Rad17 in human) in budding yeast. Elg1 (enhanced levels of genome instability), a RFC homolog, which forms an alternative RFC complex with Rfc2–Rfc5, was discovered through budding yeast genome-wide synthetic genetic interaction screening of mutants of replication fork-progression genes (11) and through the study of mutants exhibiting high levels of Ty recombination (12, 13). The Elg1 complex is distinct from RFCs for DNA replication, the DNA damage checkpoint, and sister chromatid cohesion (11–14). We have now isolated the mammalian *FRAG1* gene, characterized the function of Frag1 protein in higher eukaryotes, compared it with homologous DNA replication and damage response proteins of simpler organisms, and shown that it is involved in a Rad9-related damage checkpoint, a pathway that is important in determining whether DNA damage will be tolerated or whether the damaged cells will be eliminated by apoptosis.

Materials and Methods

Cell Culture. For synchronization by double thymidine block, after culture in medium with 10% FCS/DMEM containing 2.5 mM thymidine for 24 h (the first block), cells were washed with PBS, grown for 10 h in fresh DMEM/10% FCS, cultured 16 h in 2.5 mM thymidine (the second block) and then incubated as indicated without thymidine. Flow cytometric analysis after BrdUrd incorporation showed that >90% cells entered S phase 2–8 h after release. Cell viability was assessed by visualization of cell morphology, trypan blue, or erythrosine B exclusion, Hoescht 33342 vital staining, and flow-assisted cytometric analysis.

Genotoxic Stress and Colony Assay. For synchronized cells, 0.4 μM aphidicolin (Sigma) in 0.2% DMSO was included in the thymidine medium for 16 h of the second synchronization. Medium was exchanged for thymidine-free medium containing 2.2 μM caffeine (Sigma) and 0.4 μM aphidicolin for an indicated period. For DNA

Abbreviations: MEF, mouse embryonic fibroblast; MMS, methyl methanesulfonate; RFC, replication factor C; siRNA, short interfering RNA.

Data deposition: The sequences reported in this paper have been deposited in the GenBank database (accession nos. AY557610 and AY557611).

**To whom correspondence should be addressed at: Comprehensive Cancer Center, Ohio State University, Wiseman Hall, Room 385L, 410 West 12th Avenue, Columbus, OH 43210. E-mail: carlo.croce@osumc.edu.

damage, the DNA alkylating agent methyl methanesulfonate (MMS) (15) was added in the medium at indicated conditions. For UV irradiation, 60–70% confluent monolayer cells were irradiated with UV-C emitted by germicidal lamps (GL-15, NIPPO Electronic, Tokyo, Japan) emitting at predominantly 254 nm. For colony assay, cells were cultured in medium with MMS for 1 h, washed, and plated in DMEM/10% FBS with 1.5% methylcellulose; colonies were counted 10 days later. For radiation, cells were exposed to ^{137}Cs [661 keV (1 eV = 1.602×10^{-19} J) at indicated doses] and assessed as indicated.

Plasmids and Small Interfering RNAs (siRNAs). pcDNA4V5 DNA (Clontech), was ligated in-frame with F1 (nucleotide positions from the first coding methionine, 1–1440), F2 (1400–1839), F3 (1794–3177), F4 (2697–3975), or FZ (3972–5535) DNA fragments of human Frag1 cDNA. Wild-type pBJF-FLAG-ATR (pBJF-FLAG-ATRwt), kinase-dead pBJF-FLAG-ATR (pBJF-FLAG-ATRkd) [from S. Schreiber (Harvard University, Cambridge, MA) and K. Cimprich (Stanford University, Stanford, CA)], HA-Rad9, Flag–N-terminally deleted Rad9 [Rad9-δN; from H-G. Wang (University of South Florida, Tampa)], and pCAGGS-hbcl-2 [from Y. Eguchi and Y. Tsujimoto (Osaka University, Osaka, Japan)] were used for transfection. GST-fusion (Amersham Pharmacia) was used for protein expression.

Construction of siRNA-expression plasmids was based on the U6 siRNA expression vector (Takara, Mie, Japan), which includes a mouse U6 promoter, a puromycin-resistance gene, and two BspMI sites. Two sets of the sense and antisense oligonucleotides (Table 1, which is published as supporting information on the PNAS web site) were annealed and ligated into the vector. U6 siRNA-Frag1 plasmids were transfected into cells by using TransIT-TKO transfection reagent (Mirus, Madison, WI) and selected in 1 μg/ml puromycin. Colonies were picked, and expression was evaluated by RT-PCR and immunoblot analysis. siRNA expression vectors with EGFP antisense or without inserts were used as controls (Takara). Oligo siRNAs for mouse p73, Atr, and luciferase were used as recommended (Santa Cruz Biotechnology).

cDNA Isolation and RNA Analysis. RNAs were extracted with a Qiagen (Valencia, CA) kit and cDNAs synthesized from 2 μg of poly(A)$^+$ RNA with Superscript II reverse transcriptase and oligo(dT) and random primers (Invitrogen). Differentially expressed genes were isolated with a cDNA subtraction kit (Clontech). After two rounds of hybridizations, cDNAs were amplified, ligated to vector, and sequenced.

For hybridization, 5-μg RNAs were fractionated by agarose gel electrophoresis, transferred to Nylon membrane, and hybridized with the following probes: cDNAs of the peptide coding region of *FRAG1* (N- and C-terminal), *RFC1*, *CTF18*, *DCC*, and *RAD17*, which were amplified by RT-PCR, subcloned, and sequenced. Filters were washed and exposed to x-ray film.

Protein Analysis and Fractionation. For immunoprecipitation, cells were harvested and 500-μg samples of cell lysates, after being precleared with protein G-Sepharose beads, were incubated with 3–4 μg of specific antibody overnight. Antigen–antibody complex was immobilized on protein G-Sepharose beads, and the beads were washed five times in lysis buffer. Bound proteins were eluted by boiling and subjected to SDS/PAGE and immunoblotting. Immunofluorescence staining and confocal analysis were performed by culturing cells in chambered slides, followed by methanol fixation, 0.05% Triton X-100 treatment, and staining with first and secondary antibodies. Primary antibodies used were anti-human p53 (BD Biosciences), phosphorylated p53 (Ser-15) (BD Biosciences), Mdm2 (Santa Cruz Biotechnology), Rb (BD Biosciences), Rad9 (Santa Cruz Biotechnology), phospho-H2AX (catalog no. 07-164; Upstate Biotechnology, Chicago), mitochondria (Chemicon), Bax (catalog no. 2772, Cell Signaling Technology; N-20, Santa Cruz Biotechnology), Atr (ab-2, EMD Biosciences, San Diego; catalog no. sc-1887, Santa Cruz Biotechnology), Orc2 (BD Biosciences), cytochrome *c* (Pharmingen), phospho-H2AX (catalog no. 05-636; Upstate Biotechnology), Grb2 (BD Biosciences), V5 (Invitrogen), Flag (Sigma), and actin (ICN, Irvine CA), which were detected with secondary antisera in an enhanced chemiluminescence system (ECL, Amersham Biosciences). Rabbit polyclonal anti-Frag1 antiserum was developed against peptide sequences mouse 345 CSLSDPENEQPVQKRKSN 362 and affinity-purified. *In vitro* transcription/translation was performed with a rabbit reticulocyte system (Amersham Biosciences) by labeling cDNAs cloned by RT-PCR amplification with [^{35}S]methionine (Amersham Biosciences). Proteins were incubated in 100 μl of binding buffer containing 150 mM NaCl, 0.1% Tween 20, 0.75 mg/ml BSA, 50 mM Tris·HCl (pH 8.0), 5 mM EDTA, and 10% (vol/vol) glycerol. For pulling down, glutathione–agarose bead-bound proteins were subjected to SDS/PAGE after being washed five times, and the gels were exposed to x-ray film. Cellular fractions were prepared as described in ref. 16.

Results and Discussion

Identification of FRAG1, a Gene Differentially Expressed After Replication Stress. DNA replication guarantees the duplication of the genome and requires concerted, dynamic changes of expression of specific gene products, which regulate the integrity of replication and surveillance of the genome for damage (17). When replication forks encounter damage in the DNA strands, stalling or arrest can result, leading to stimulation of the downstream checkpoint to initiate cell cycle arrest or apoptosis (1); however, the molecular mechanisms that sense stalled replication are not understood fully. To study differentially expressed genes in conditions of replication stress, synchronized mouse embryonic fibroblasts (MEFs) were exposed to aphidicolin, a DNA polymerase inhibitor, and harvested 4 h (in mid-S phase) after release from a double thymidine block. RNA was extracted from MEFs, and subtractive cDNA hybridization was performed to identify genes differentially expressed in the presence or absence of aphidicolin (Fig. 7*A*, which is published as supporting information on the PNAS web site). BLAST database searches indicated that 155 clones that we isolated and sequenced included 86 clones (55%) identical to mouse ESTs (>95% homologous over 200 bp). The 86 clones included redundant clones; 13 clones corresponded to an overlapped cDNA contig (denoted as FRAG1/N), seven clones corresponded to a contig (FRAG1/C), and five clones corresponded to *RFC1* cDNA. Interestingly, database searches indicated that FRAG1/N and FRAG1/C are located adjacent to each other (C130052G03Rik, GenBank accession no. XM_282980; Gm17, GenBank accession no. XM_111221) on mouse chromosome 11. Database searches for human orthologs of the mouse clones showed that the orthologs are parts of a continuous gene, FLJ12735 (GenBank accession no. NM_024857), at human chromosome 17q11.2. RT-PCR amplification indicated that those "two" mouse transcripts span a gene, suggesting that the two transcripts, FRAG1/N and FRAG1/C came from one gene, *FRAG1* (Ctf18/Rad24/Elg1-related gene 1). We have focused on characterization of the *FRAG1* gene.

Alteration of FRAG1 Expression. Northern blot analysis was performed with replication-related genes *RFC1*, *RAD17*, and *CTF18*, as well as FRAG1/N and FRAG1/C as probes. Synchronized MEFs were treated with aphidicolin or MMS (a DNA alkylating agent), agents that cause stalled DNA replication (15). Expression of FRAG1/N and FRAG1/C was markedly down-regulated by aphidicolin or MMS treatment, whereas the effect on *RFC1*, *Rad17*, and *CTF18* genes was less apparent after MMS treatment (Fig. 1*A*). RNA blot with cDNA probes of N- and C-terminal portions of *FRAG1* (FRAG1/N and FRAG1/C) (Fig. 1*C*) detected a predominant transcript of ≈9 kb expressed ubiquitously in 12 murine cell lines (Fig. 1*B*). To assess the stability of the *FRAG1* transcript,